Space Sci Rev (2015) 191:27–76
DOI 10.1007/s11214-015-0143-1

Observations of Strong Magnetic Fields in Nondegenerate Stars

Jeffrey L. Linsky[1] · **Markus Schöller**[2]

Received: 22 November 2014 / Accepted: 4 March 2015 / Published online: 14 March 2015

Abstract We review magnetic-field measurements of nondegenerate stars across the Hertzprung–Russell diagram for main sequence, premain sequence, and postmain sequence stars. For stars with complex magnetic-field morphologies, which includes all G–M main sequence stars, the analysis of spectra obtained in polarized vs unpolarized light provides very different magnetic measurements because of the presence or absence of cancellation by oppositely directed magnetic fields within the instrument's spatial resolution. This cancellation can be severe, as indicated by the spatially averaged magnetic field of the Sun viewed as a star. These averaged fields are smaller by a factor of 1000 or more compared to spatially resolved magnetic-field strengths. We explain magnetic-field terms that characterize the fields obtained with different measurement techniques. Magnetic fields typically control the structure of stellar atmospheres in and above the photosphere, the heating rates of stellar chromospheres and coronae, mass and angular momentum loss through stellar winds, chemical peculiarity, and the emission of high energy photons, which is critically important for the evolution of protoplanetary disks and the habitability of exoplanets. Since these effects are governed by the star's magnetic energy, which is proportional to the magnetic-field strength squared and its fractional surface coverage, it is important to measure or reliably infer the true magnetic-field strength and filling factor across a stellar disk. We summarize magnetic-field measurements obtained with the different observing techniques for different types of stars and estimate the highest magnetic-field strengths. We also comment on the different field morphologies observed for stars across the H–R diagram, typically inferred from Zeeman-Doppler imaging and rotational modulation observations.

✉ J.L. Linsky
jlinsky@jila.colorado.edu
Fax: +1-303-492-5235

M. Schöller
mschoell@eso.org
Fax: +49-89-32006-530

[1] JILA/University of Colorado and NIST, Boulder, CO, USA

[2] European Southern Observatory, Garching, Germany

Keywords Magnetic fields · Pre-main sequence stars · Main sequence stars · Post-main sequence stars

List of Acronyms and Abbreviations

BBLP	Broad-band linear polarization
BOB	B fields in OB stars consortium
CFHT	Canada-France-Hawaii Telescope
CP	Chemically preculiar A- and B-type stars
CRIRES	CRyogenic high-resolution InfraRed Echelle Spectrograph
DI	Doppler imaging
ESO	European Southern Observatory
ESP_aDO_nS	a high-resolution spectrograph on the CFHT telescope
FEROS	Fiber-fed Extended Range Optical Spectrograph
FORS1	FOcal Reducer and low dispersion Spectrograph
FORS2	New version of FORS1
FUV	Far ultraviolet (912–1700 Å)
GTO	Guaranteed time observer
HARPS	High Accuracy Radial Velocity Planet Searcher
HARPSpol	HARPS with polarizing optics
HINODE	Solar-B satellite
IVQU	Components of the Stokes polarimetry vector
LTE	Local thermodynamic equilibrium
LSD	Least-squares deconvolution
MDI	Michelson Doppler imager
MHD	Magnetohydrodynamics
MiMeS	Magnetism in Massive Stars collaboration
MOST	Microvariability and Oscillations of STars satellite
NIM	Near Infrared Magnetograph
NSO	National Solar Observatory
RGB	Red giant branch stars
SB	Spectroscopic binary stars
SOFIN	An optical high-resolution spectrograph on the Nordic Optical Telescope
SOHO	Solar and Heliospheric Observatory
SOT	Solar Optical Telescope
SOT/SP	SOT Spectropolarimeter
SPB	Slowly pulsating B-type stars
SVD	Singular value decomposition method for Stokes profile reconstruction
UV	Ultraviolet (912–3000 Å)
VLT	Very Large Telescope
ZAMS	Zero-age main sequence
ZDI	Zeeman Doppler imaging

1 Introduction and Terminology

A prominent solar physicist once remarked,

> "If the Sun did not have a magnetic field, it would be as uninteresting as most astronomers consider it to be."

Table 1 Magnetic field terminology

Measurement type	Spatially unresolved observations	
	Filling factor included	Filling factor separate
Stokes I unsigned line-of-sight spectra (no cancellation)	Mean unsigned magnetic-field strength (or flux density) (unpolarized Zeeman broadening) $\langle B \rangle = B_{\rm MOD} f$	Unsigned magnetic-field modulus and filling factor (unpolarized Zeeman splitting) $B_{\rm MOD}$ and f
Stokes V or IVQU signed line-of-sight spectropolarimetry (with cancellation)	Net longitudinal magnetic-field strength (or flux density) (Zeeman broadening) $\langle B_z \rangle = B_{\rm NET} f$	Net magnetic-field modulus and filling factor (Zeeman splitting) $B_{\rm NET}$ and f

Such statements about the Sun and stars in general ignore the important ways in which magnetic fields typically control the structure of stellar atmospheres in and above the photosphere, the heating rates of stellar chromospheres and coronae, mass and angular momentum loss through stellar winds, chemical peculiarity, and the emission of high energy photons, which is critically important for the evolution of protoplanetary disks and the habitability of exoplanets. Thus, stellar structure models and phenomenological descriptions are woefully incomplete without a clear picture of the star's magnetic-field morphology and variability. Here we will summarize the magnetic-field measurement techniques, observations, and phenomena of nondegenerate stars. For other summaries of this topic, see the review papers by Reiners (2012) and Donati and Landstreet (2009). For a review of theoretical ideas that have been proposed to explain the origins and morphologies of magnetic fields in nondegenerate stars, see the following chapter where Ferrario et al. (2015) provide an overview of turbulent dynamo theories including a description of the inverse cascade of magnetic energy to large scales and the back reaction of strong fields leading to saturation. Also see the review by Donati and Landstreet (2009) and references therein and the recent papers by Nelson et al. (2013, 2014) on solar-like dynamos.

Before proceeding, it is essential to understand magnetic-field terminology (see Table 1). Unfortunately, these terms are often misapplied, which makes it difficult to compare theory with observations and to identify the strongest magnetic fields on the stellar surface.

Vector Magnetic-Field Strength $\mathbf{B}(\mathbf{x}, t)$ is the true strength of the local magnetic-field vector at a given location and time in the stellar photosphere (see Fig. 1). Although this is an essential quantity that must be compared with theory, it is very difficult to measure. There are very few measurements of $\mathbf{B}(\mathbf{x}, t)$ on the Sun (e.g., Rabin 1992) and, except for stars with the simplest magnetic-field morphologies, none for stars because magnetographs have apertures that are not able to resolve magnetic fields that are inhomogeneous on small spatial scales. Many magnetic-field measurements are polarimetric, in which case there is cancellation by oppositely directed fields. When such cancellations cannot be corrected for, we use the term net magnetic-flux density, $\mathbf{H}(\mathbf{x}, t)$ to describe the vector field with cancellation.

Mean Unsigned Magnetic-Field Strength Unpolarized spectra can be used to measure the unsigned magnetic field by studying the excess broadening of high Landé g spectral lines compared to otherwize similar low Landé g lines or by analyzing resolved line splitting when the magnetic field is strong. Since the magnetic-field strength varies across the stellar surface, it is useful to define a "mean-unsigned–magnetic-field strength", $\langle B \rangle$, which is an average value of the magnetic field across the stellar surface, and an "unsigned-magnetic-field modulus" also called the "mean magnetic-field modulus" (e.g., Hubrig et al.

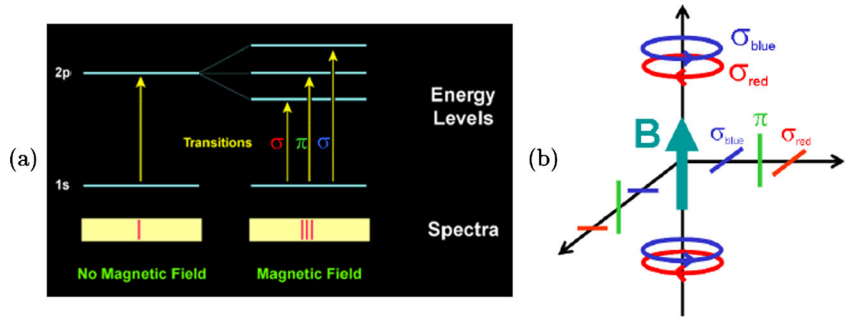

Fig. 1 *Left*: The splitting $\Delta\lambda = 46.67 g \lambda^2 B$ in mÅ of a 2p level in the presence of a magnetic field, where B is in kGauss and g is the Landé splitting factor. Since the splitting is proportional to the magnetic-field strength squared, the best opportunity for actually measuring B is with infrared instrumentation. *Right*: Circular polarization (Stokes vector V) is observed when the magnetic field is along the line of sight, and linear polarization (Stokes vectors Q and U) is observed when the magnetic field is observed perpendicular to the line of sight. Figure from Reiners (2012)

2005), $B_{\rm MOD}$, which is the peak magnetic-field strength. These two quantities are related by $\langle B \rangle = B_{\rm MOD} f$, where the filling factor f is the fraction of the stellar surface covered by $B_{\rm MOD}$. In the simplest case, one can approximate the distribution of magnetic field strengths within an instrument's field of view by a single magnetic-field strength $B_{\rm MOD}$ filling a fractional area f and zero magnetic field filling the remaining fractional area, $1 - f$. When the signal-to-noise ratio and spectral resolution are excellent, especially in the infrared where the λ^2 dependence of the σ and π component splitting resolves the Zeeman pattern, $B_{\rm MOD}$ can be measured from the wavelength difference of the split components and f can be determined by fitting the depth of the Zeeman absorption components. In a few cases, for example the measurements of the classical T Tauri star BP Tau by Johns-Krull et al. (1999), observers have been able to identify a distribution of magnetic-field strengths with corresponding filling factors, such that $B_{\rm MOD} f = \sum_i B_{{\rm MOD},i} f_i$. When the magnetic field is too weak to resolve the splitting of the Zeeman components, one can measure only $\langle B \rangle = B_{\rm MOD} f$.

Net Longitudinal Magnetic-Field Strength Spectropolarimeters measure net magnetic fields produced by the cancellation of oppositely oriented magnetic fields subtended within the instrument's field of view—either the observed stellar hemisphere, the resolution element obtained with Zeeman Doppler-imaging observations (see below), or the spatial resolution element on the Sun. We use the term "net longitudinal magnetic-field strength", $\langle B_{\rm z} \rangle$, to refer to the magnetic field averaged over the spatial resolution element of the detector on the Sun or the entire star, including field cancellation. We refer to the peak signed magnetic field in the resolution element as the "net magnetic-field modulus", $B_{\rm NET}$, which is the largest signed magnetic field strength seen anywhere on the solar surface away from sunspots or at any rotational phase of a star. The relation between these two quantities is $\langle B_{\rm z} \rangle = B_{\rm NET} f$, where f is the filling factor.

Since stellar magnetic fields are often complex on small spatial scales, unpolarized instruments measure $\langle B \rangle$, which for stars with complex magnetic-field morphologies like the Sun is much larger than the net longitudinal field $\langle B_{\rm z} \rangle$. For stars with simple dipolar fields like many of the Ap stars, these two quantities can be similar. Both instruments with and without polarizing optics have great difficulty identifying the contribution of the strongest magnetic fields, which typically occur in dark starspots, when measuring unresolved stellar

emission. The presence of strong magnetic fields in dark starspots has only been measured on the Sun with high-resolution infrared instruments as we will show. For all other observations of the Sun and stars, instruments measure a magnetic quantity that is smaller, and often much smaller, than the highest value of $\mathbf{B}(\mathbf{x}, t)$.

2 Techniques for Measuring Magnetic Fields

In this section, we discuss magnetic field observations obtained by four direct and three indirect techniques. For additional discussion of this topic see Reiners (2012) and Donati and Landstreet (2009).

Net Circular Polarization This is the classical technique used for more than 100 years to measure net longitudinal magnetic-field strengths, $\langle B_z \rangle$. The magnetic signal is provided by the difference between opposite circular- polarization spectra (blue–red in Fig. 1) for a spectral line with a large Landé g factor. The required instrumentation is relatively simple, but oppositely directed fields cancel within a spatial resolution element. Also, since these measurements are only sensitive to the longitudinal component of the magnetic-field vector, they refer to the net magnetic-field strength rather than the vector magnetic-field strength, $\mathbf{B}(\mathbf{x}, t)$. Since circular polarization is not sensitive to nonmagnetic line broadening, this technique can measure weak magnetic fields. However, signal saturation when measuring strong magnetic fields can limit the range of measurable fields. When observing stars with largely organized magnetic fields, such as the chemically peculiar stars, measurements of $\langle B_z \rangle$ are invaluable tools to learn about the net magnetic-field modulus, $B_{\rm NET}$, and the magnetic topology, since the magnetic field changes in a characteristic way while the star rotates.

Zeeman Broadening Spectral lines with large Landé g factors are broadened more than lines with small g factors. The excess broadening of a high g line compared to a low g line provides a measure of the unsigned magnetic-field strength averaged over the stellar hemisphere, $\langle B \rangle$. However, the high and low g lines must have nearly the same broadening, except for the magnetic component, as likely occurs for two spectral lines of similar strength formed in the same region of the atmosphere and preferably from the same element or ion. This technique first developed by Robinson et al. (1980) requires only high-resolution spectra obtained without polarizing optics. Since many effects can broaden a spectral line, this technique works best for measuring strong magnetic fields.

Zeeman Splitting When high-resolution spectroscopy in the infrared makes it feasible, the resolved σ components of an absorption line provide a measurement of the average value of $\langle B \rangle$ over the stellar surface or observed region on the Sun. For the strong magnetic fields of the Ap stars, Zeeman splitting is also observed in the visible.

Zeeman Doppler Imaging The Doppler-imaging (DI) technique provides relative brightness images of the surface of a rotating star in a spectral line. At each rotational phase, the bright and dark regions along each stellar longitude modify the spectral line profile at their corresponding Doppler shifts. Analysis of high-resolution spectra obtained at many rotational phases lead to a synthetic stellar image with the bright and dark regions displayed at their proper locations across the stellar surface. The Zeeman Doppler-imaging (ZDI) technique provides magnetic-field maps of the stellar surface with comparable spatial resolution. Instruments that measure circular polarization (i.e., Stokes vector V, which is proportional to

$\langle B_z \rangle$) provide stellar surface maps of $B_{\rm NET} f$. Instruments that measure both circular and linear polarization (i.e., Stokes vectors QU, which are proportional to the transverse magnetic field) provide surface maps of the radial, toroidal, and meridional components of $B_{\rm NET} f$. This technique is described in detail by Donati and Landstreet (2009). Since the spectral resolution set by the rotation rate and the spectral resolution cannot resolve the small scale structure of $\mathbf{B}(\mathbf{x}, t)$, such instruments measure the vector or longitudinal components of the net magnetic-flux density, $\mathbf{H}(\mathbf{x}, t)$.

Nonthermal Radio Emission Active late-type stars are often detected by their gyrosynchrotron radio emission produced by relativistic electrons spiraling in coronal magnetic fields. Observations over a wide spectral range can provide estimates of the coronal magnetic-field strength. Inactive stars like the Sun emit gyroresonance emission produced by thermal electrons spiraling in coronal magnetic fields. The wavelength of third-harmonic gyroresonant emission from solar active regions provides an accurate measure of coronal magnetic-field strengths.

Sunspots and Starspots Optical solar images show dark sunspots and bright faculae in the photosphere. Magnetic-field measurements in sunspots show the strongest magnetic fields on the solar surface and similar measurements in bright faculae show moderate-strength fields. Dark sunspots are generally thought to be produced by magnetic suppression of convective energy transport, and the bright faculae are typically explained by magnetic heating in the low chromosphere. Doppler images and rotational modulation studies provide evidence for very large starspots in active stars, providing an indirect indicator of magnetic fields.

Indicators of Magnetic Heating Stellar chromospheres ($T = 10^4$–10^5 K) and coronae ($T \geq 10^6$ K) are generally thought to be heated by either the dissipation of magnetohydrodynamic (MHD) waves or the direct conversion of magnetic to kinetic energy (microflaring). Both mechanisms involve magnetic fields, and the hotter outer layers produce emission lines of Ca II, hydrogen (H-α and Lyman-α), and many highly ionized species in the UV and X-ray spectra. These emission features provide strong evidence for the presence of magnetic fields but do not measure magnetic-field strengths.

3 What can be Learned from a Spatially Resolved Star, the Sun?

By virtue of its proximity and brightness, the Sun provides the best laboratory for studying magnetic fields on a star, but even for this special case there are important limitations. Figure 2 shows a high-resolution magnetogram of the whole Sun and an expanded portion near disk center obtained with the Michelson Doppler Imager (MDI) on the Solar and Heliospheric Observatory (SOHO) spacecraft. The figure shows the net longitudinal magnetic-field strength, $\langle B_z \rangle$, obtained with the circular polarization- differencing technique by observing the Ni I 6768 Å line with a Landé $g = 1.43$. With $2'' \times 2''$ pixels, MDI could not measure unsigned magnetic-field strengths as the magnetic-field morphology is inhomogeneous on smaller spatial scales. Since the largest $\langle B_z \rangle$ values shown in this figure are ± 250 G, the maximum resolved magnetic-field strengths, $B_{\rm MOD}$, must be much larger. How much larger? To answer this question, we consider another observing technique.

For Zeeman-sensitive lines with large Landé g factors observed in the infrared, the wavelength-splitting pattern obtained when opposite circular-polarization spectra are subtracted is larger than the linewidth. In this case, the observed splitting is proportional to the

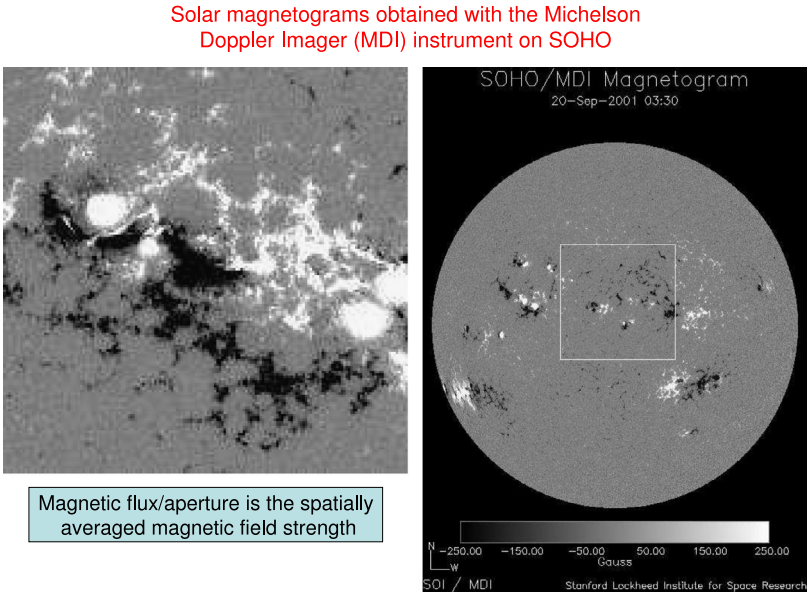

Fig. 2 Magnetic-flux densities of the whole Sun (*right*) and the center of the solar disk (*left*) obtained by the MDI instrument on the Solar and Heliospheric Observatory (SOHO) spacecraft with a resolution of 2″. *White* and *black* refer to opposite orientations of the net longitudinal magnetic-field strength

net magnetic-field strength modulus, $B_{\rm NET}$, and the amplitude of the circular polarization signal indicates the approximate filling factor of the magnetic field in the solar photosphere at this spatial resolution. Rabin (1992) used this Zeeman-splitting technique to measure the distribution of magnetic fields in a solar active region by observing the Fe I 1.565 μm line. The distribution shown in Fig. 3 has a peak near $B_{\rm NET} = 1300$ Gauss with a width of 270 Gauss. Rabin estimated that the filling factor for the 1300 Gauss field is $f = 0.1$–0.2, implying that $\langle B_{\rm z}\rangle = B_{\rm NET}\, f$ should be approximently 130–260 Gauss. By comparison, the distribution of net longitudinal magnetic-field strengths measured in the optical spectrum with the National Solar Observatory (NSO) magnetograph in the same active region at the same time ranges between 0 and 500 Gauss with most resolution elements showing $\langle B_{\rm z}\rangle \leq 250$ Gauss. Since both instruments had similar spatial resolution of 2", the two data sets are consistent. This comparison suggests that magnetic flux measurements without independent estimates of f would underestimate the magnetic-field modulus by a factor of 5–10, even for the high spatial-resolution observations of the Sun. The lack of spatial resolution for stellar observations suggests that there is an even larger discrepancy between $B_{\rm NET}$ and $\langle B_{\rm z}\rangle$ for stars.

The Solar Optical Telescope/Spectropolarimeter (SOT/SP) on the *HINODE* satellite provides 0.″32 angular resolution and 10^{-3} polarization sensitivity. Viticchié et al. (2011) have inverted a representive sample of these Stokes V data with a code that allows for unresolved magnetic elements smaller than even this extremely high resolution. They found a distribution of net magnetic-field modulus values with the largest fraction of the observed field at $B_{\rm NET} = 1600$ Gauss. They also found that 95.5 % of their observed region in the photosphere had no, or very weak, magnetic fields such that the $\langle B_{\rm z}\rangle = 66$ G. This analysis provides a picture of the nearest star in which photospheric magnetic fields are concentrated in very thin flux tubes with a distribution of field strengths up to 1600 Gauss. Such stars occupy a

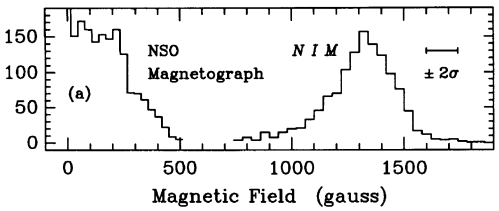

Fig. 3 Plotted on the right is the histogram (y axis) of the net magnetic-field modulus, B_{NET}, measured in a solar active region by the Near Infrared Magnetograph (NIM). The λ^2 splitting of the Zeeman σ components permits measurements of true magnetic field strengths in the infrared. Plotted on the left is the histogram (also y axis) of the net-longitudinal magnetic-field strength (also called flux density), $\langle B_{\mathrm{z}} \rangle$, in the same active region observed at the same time by the National Solar Observatory (NSO) magnetograph. The x-axis plots the corresponding magnetic-field strengths measured in the two different ways. The NIM was able to measure B_{NET} values from the complete splitting in Stokes V spectra of the Fe I 1.565 μm line with Landé $g = 3.00$, whereas the NSO magnetograph observing in the optical could not detect the splitting of spectral lines in Stokes V, resulting in field cancellation and averaging of the inhomogeneous field. Figure from Rabin (1992)

very small fraction of the photosphere at its base, and then rapidly decrease with height as the flux tubes expand. If this picture of the solar magnetic-field morphology is representative of other convective stars, then from measurements of stellar mean magnetic-field strengths (signed or unsigned) it will be very difficult to infer magnetic modulus values, filling factors, and magnetic energies.

The strongest solar magnetic fields are found in sunspot umbrae. Moon et al. (2007) analyzed Stokes IVQU spectra of the Fe I 6301.5 Å line observed in a sunspot umbra with the SOT/SP instrument on *HINODE*. In these 0.″6 resolution spectra, they found maximum net field strengths of about 4500 Gauss. These field strengths are about 1000 Gauss stronger than typical ground-based measurements (e.g., Pevtsov et al. 2014) likely because of the absence of spartial smearing due to seeing and minimal scattered light in the SOT/SP data.

Measuring the net longitudinal magnetic field of the Sun viewed as an unresolved point source by a distant observer can be done by studying the solar spectrum reflected by an asteroid or by integrating whole disk magnetograms. An example of the first approach is the study of the solar spectrum reflected by Vesta that Daou et al. (2006) found to have $\langle B_{\mathrm{z}} \rangle = -4 \pm 3$ Gauss. This is a very small net field compared to the active stars described below. An example of the second approach is the measurement by Plachinda et al. (2011) who found $\langle B_{\mathrm{z}} \rangle = \pm 2$ Gauss at the maximum of the solar activity cycle and ± 0.2 Gauss at the minimum. Schrijver and Liu (2008) found total magnetic fluxes of 25×10^{22} Maxwells at times of solar minima and 100×10^{22} Maxwells at the maxima of the sunspot cycle by integrating global magnetograms obtained with the SOHO/MDI instrument. For comparison, individual active regions on the Sun have magnetic fluxes in the range 10^{20} to 3×10^{22} Maxwells. For a more detailed description of the solar magnetic field see, for example, Schrijver and Zwaan (2000).

4 Pre-Main Sequence Stars

Magnetic fields play key roles in essentially all aspects of the star formation process (e.g., McKee and Ostriker 2007). Models of magnetically driven accretion and outflows successfully reproduce many observational properties of low-mass pre-main sequence stars, also called young stellar objects (YSOs). While indirect observational evidence for the presence of magnetic fields in these stars is manifested in strong X-ray, FUV (912–1700 Å), and UV

(912–3000 Å) emission, flaring, and gyrosynchrotron radio emission (e.g., Feigelson and Montmerle 1999), there are now many direct observations of YSO magnetic fields.

4.1 T Tauri Stars

The evolution of YSOs from dense clumps of interstellar gas and dust to main sequence stars proceeds through several stages (Feigelson and Montmerle 1999). The earliest phase of a protostar (referred to as a Class 0 object) consists of a collapsing massive disk detectable only at millimeter and far-infrared wavelengths. After about 10^5 years, the collapsing cloud has formed a Class I object consisting of a heavily obscured star heated by the release of gravitational energy and a large circumstellar disk. After about 10^6 years, the star becomes optically visible above and below the plane of the disk, although the visible spectrum is veiled by emission from the disk. These stars are called Classical T Tauri stars (CTTSs) or Class II objects. Strong UV emission seen in CTTSs results mostly from accretion of gas along magnetic field lines from the disk to the star, producing postshock regions with strongly enhanced emission in the He I λ5876 and other lines. Strong X-ray emission can be produced in the postshock region, closed-field lines in the stellar corona, and where stellar and disk magnetic fields interact. In the last stage of evolution to the main sequence, which occurs between a few million years and 10^7 years, most of the gas and dust from the disk has condensed into planets or has been accreted onto the star, which is now called a Weak-lined T Tauri star (WTTS) or Class III object. WTTSs are often called naked TTSs because their ultraviolet emission line spectrum is no longer obscured by a disk.

Zeeman broadening of infrared absorption lines provides a powerful tool for measuring the unsigned magnetic-field strengths, $\langle B \rangle$, of CTTSs. Johns-Krull (2007) summarized previous studies and included new measurements for 15 CTTSs (mostly spectral types K7–M2) in the ∼2 Myr old Taurus region. Analysis of spectropolarimetry of four Ti I lines at wavelengths near 2.2 μm allowed him to solve for the distribution of field strengths and their sum to obtain $\langle B \rangle$. These field strengths do not correlate with the predictions of several magnetospheric models and are typically twice as large as predicted by pressure equilibrium with the photospheric gas, unlike the case for main sequence stars. He argued that the need for horizontal pressure balance requires that strong fields must cover the entire stellar surface of CTTSs. Since spectropolarimetric measurements (see below) indicate much weaker fields for these stars, the fields needed for horizontal pressure balance must have complex morphologies rather than be simple inclined dipoles. These strong complex fields are dynamo-driven in the stellar convective zone starting from "seed" primordial fields. The role of strong magnetic fields in controlling the accretion flow from disks to small areas at high latitudes on the stellar surface is now generally accepted, see the review by Bouvier et al. (2007). The Reiners (2012) review paper includes an updated list of Zeeman-broadening measurements for pre-main sequence stars.

The Zeeman-broadening technique has permitted Johns-Krull and collaborators to sample the unsigned magnetic fields of pre-main sequence stars with a range of ages younger and older than the CTTSs in Taurus. Johns-Krull et al. (2009) obtained the first measurement of the magnetic-field strength of a Class 1 protostar WL 17. They obtained $\langle B \rangle = 2.9 \pm 0.43$ kG, which corresponds to three times the photospheric gas pressure indicating that the entire photosphere of this embedded $\sim 10^5$ yr protostar is likely dominated by strong fields. Yang and Johns-Krull (2011) studied 14 Class II CTTSs (spectral types K3–M1.5) in the 1 My old Orion Nebular Cluster. These stars have measured $\langle B \rangle$ between 1.3 and 3.45 kG with magnetic pressures about twice that of the photospheric gas pressure. The ∼10 Myr old TW Hya association contains stars at the very end of the pre-main sequence

phase. Using the same observational technique, Yang et al. (2008) found that magnetic fields of five Class III naked TTSs with spectral types K7–M3 have $\langle B \rangle = 3.1$–4.9 kG. For these stars the photospheric magnetic pressure also dominates the gas pressure. Comparing the magnetic fields of the youngest to the oldest pre-main sequence stars, Yang and Johns-Krull (2011) found no dependence on age for the unsigned magnetic-field strength but a systematic decrease in the magnetic flux ($4\pi R_\star^2 \langle B \rangle$) with age as a result of the systematic decrease of stellar radius with age.

Spectropolarimetry provides the basis for mapping the topological structure of large-scale magnetic fields of pre-main sequence stars. While the magnetic fields of many CTTSs have now been mapped, the 1.5 Myr star BP Tau observed by Johns-Krull et al. (1999), Donati et al. (2008b), and Chen and Johns-Krull (2013) provides an illustrative example. All three studies found that the circular polarization seen in the He I λ5876 and several other emission lines, which are produced in postshock accretion regions, occur in very small areas (2–3 % of the stellar surface) generally located at high latitudes. The longitudinal magnetic field strength in BP Tau's accretion region was measured by Johns-Krull et al. (1999) to be $\langle B \rangle = 2460 \pm 120$ G by the Zeeman-broadening technique but as large as 12 kG by Donati et al. (2008b) using the ZDI technique. The reason for this large discrepancy is uncertain. The correspondence of Stokes I and Stokes V images led Donati et al. (2008b) to conclude that the accretion region overlies a large dark starspot in the photosphere near the star's rotational pole. All three studies agree that the dark starspot covers about 25 % of the visible surface and that the remainder of the star is threaded with strong, but tangled, magnetic fields with an unsigned magnetic field strength $\langle B \rangle = 2.6 \pm 0.3$ kG, but only an upper limit to the mean longitudinal magnetic field measured by differencing absorption line profiles in opposite circular polarizations. Donati et al. (2008b) found that a simple approximation to the magnetic-field topology is the sum of tilted dipole and octopole components, but only 90 % of the large scale magnetic energy is poloidal, with the remainder torroidal. Since the measured magnetic-field strength exceeds pressure equilibrium with the photospheric gas, the entire surface must be covered by strong radial or complex magnetic fields. According to Donati et al. (2008b), the strong fields are likely produced by dynamo processes in the star's convective zone rather than being primordial.

Donati and an international team of collaborators have nearly completed the Magnetic Protostars and Planets (MaPP) project to map the surface brightness and magnetic-field topology of 15 CTTSs using the ESPaDOnS spectropolarimeter on the 3.6 m Canada-France-Hawaii Telescope and the NARVAL spectropolarimeter on the 2 m Télescope Bernard Lyot. The observed CTTSs include the very low mass 0.35 $M_\odot$ star V2247 Oph (Donati et al. 2010a) and the 0.7 $M_\odot$ CTTSs DN Tau (Donati et al. 2013) and AA Tau (Donati et al. 2010b), which like BP Tau have fully convective interiors. Their observing program also includes the higher mass stars TW Hya (Donati et al. 2011) and the 1.7–1.8 $M_\odot$ stars CV Cha and CR Cha (Hussain et al. 2009), which have radiative cores. The CTTSs range in age from about 1.5 Myr [AA Tau, BP Tau, and V2247 Oph (Donati et al. 2010a)] to about 8 Myr (TW Hya). Figure 4 plots the luminosities and effective temperatures for these and other CTTSs and identifies their locations along pre-main sequence evolution tracks for their masses. The basic properties of large-scale magnetic fields of CTTSs shown in Fig. 4 suggest that these properties may change as stars develop a radiative core. However, this suggestion is based on only two stars (V4046 Sgr A and B) and there are many competing effects including spin-down with mass loss and spin-up with accretion and decreasing radius with age. More data are needed to address this question.

An important criterion for classification as a CTTS is evidence of accretion of gas from the circumstellar disk to the star. For CTTSs with dipolar magnetic fields, the footpoints of

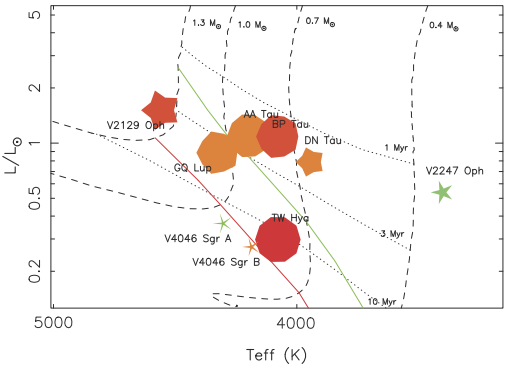

Fig. 4 The basic properties of large-scale magnetic topologies of CTTSs obtained by the ZDI technique. *Symbol size* indicates the relative magnetic intensities. *Symbol color* illustrates the magnetic-field configurations (*red* to *blue* for purely poloidal to purely toroidal fields). Symbol shape depicts the relative axisymmetry of the poloidal field component (*decagon* and *stars* for purely axisymmetric and purely non-axisymmetric poloidal fields, respectively). *Dashed lines* are pre-main sequence evolution tracks and *dotted lines* are the corresponding isochrones. CTTSs begin to develop radiative cores below the *green line* and convective envelopes become thinner than $0.5R_\star$ below the *red line*. Figure and caption from Donati et al. (2013)

accretion columns, as indicated by postshock heated emission in the He I 5876 Å, Ca II, and hydrogen lines, occur in small areas (about 2 % of the observed disk) located in high-latitude regions where strong magnetic fields overlie spots that are optically dark in the photosphere like sunspots. On the other hand, stars with very complex fields, such as the lowest mass CTTS V2247 Oph, the accretion impact area is at a range of latitudes (Johnstone et al. 2014), and the underlying photosphere may not appear to be dark. The longitudinal magnetic fields where the accretion occurs are typically in the range $\langle B \rangle = 2$–3 kG and appear to be mainly radial. These spot fields do not contribute to the average stellar magnetic field obtained from Stokes V measurements of photospheric absorption lines, because the photospheric emission from these starspots is faint.

Outside of the accretion shock regions, the stellar magnetic field can be approximated by a sum of multipoles typically misaligned with respect to the rotational pole. For many of the mapped CTTSs, the octopole component is stronger and often very much stronger than the dipole. AA Tau is an exception. In general, the more complex the geometry of the large-scale field, the weaker the dipole component and the more distributed the magnetic flux across the stellar surface (Johnstone et al. 2014). The percent of magnetic energy in the toroidal field ranges from < 5 % for the oldest star TW Hya to 50 % or more for V2247 Oph and the high mass stars V2129 Oph, CR Cha, and CV Cha. The coupling of stellar magnetic fields with magnetic fields in the inner disk slows stellar rotation, because the Keplerian rotation speed of the inner disk is generally slower than that of the star, while accretion of disk gas adds angular momentum to the star, thereby increasing its rotation rate. Hussain et al. (2009) and Donati et al. (2011) have called attention to the role that stellar radiative cores can play in this angular momentum interchange. As CTTSs age and evolve toward the main sequence, they develop radiative cores and weaker dipole fields. The effect is to weaken the star-disk magnetic coupling, allowing accretion to speed up the stellar rotation unhindered. Johnstone et al. (2014) describe the correlation of simpler magnetic-field geometry with slower rotation and larger size of X-ray-emitting stellar coronae. Vidotto et al. (2014) show that the increase in stellar rotation rates with age is consistent with the weakening of the star-disk deceleration torque with age.

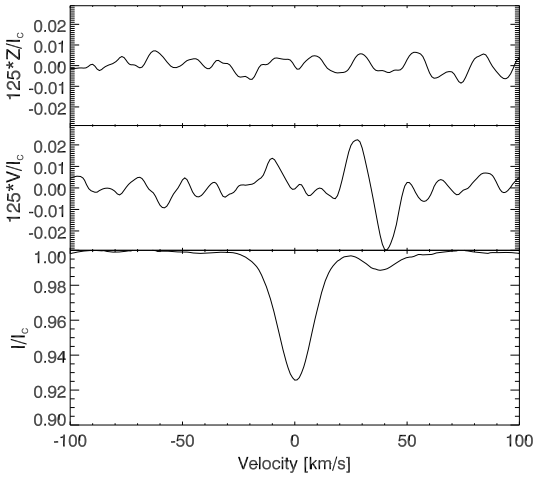

Fig. 5 Analysis of the presence of a magnetic field in both components of the Herbig Ae SB2 system HD 104237 by applying the SVD method to polarimetric spectra with the High Accuracy Radial Velocity (HARPS) instrument. The upper spectrum presents the diagnostic null (or Z) spectrum, which is associated with the Stokes V spectrum by using subexposures with identical waveplate orientation. Below the null spectrum, one finds the Stokes V and Stokes I spectra. The measured-net longitudinal magnetic field for the primary is about 13 G, while for the secondary it is 128 G

4.2 Herbig Ae/Be Stars

Magnetic fields have also been detected in half a dozen Herbig Ae/Be stars (e.g., Hubrig et al. 2009c). Similar to T Tauri stars, Herbig Ae/Be stars show clear signatures of surrounding disks as evidenced by a strong infrared excess and are actively accreting material.

Current theories are neither able to present a consistent scenario of how the magnetic fields in Herbig Ae/Be stars are generated nor how these fields interact with the circumstellar environment consisting of a combination of disk, wind, accretion, and jets. On the other hand, understanding the interaction between the central stars, their magnetic fields, and their protoplanetary disks is crucial for reconstructing the Solar System's history and accounting for the diversity of exo-planetary systems.

Before 2004, the only magnetic field detection of about 50 G had been reported for the optically brightest ($V = 6.5$) Herbig Ae star HD 104237 (Donati et al. 1997), but no further publications confirming this detection existed until recently. Using high-resolution, high signal-to-noise spectropolarimetric observations with the High Accuracy Radial velocity (HARPSpol) instrument, Hubrig et al. (2013b) detected a weak net-mean-longitudinal magnetic field. And only now have Hubrig et al. (in preparation) been able to demonstrate that the secondary component possesses a magnetic field (see Fig. 5). Spectropolarimetric studies from 2004 to 2008 reported the discovery of magnetic fields in seven other Herbig Ae/Be stars (Wade et al. 2005, 2007; Catala et al. 2007; Hubrig et al. 2004, 2006a, 2007). Later on, a study of 21 Herbig Ae/Be stars with the FOcal Reducer and low dispersion Spectrograph (FORS 1) revealed the presence of magnetic fields in six additional stars (Hubrig et al. 2009b). More recent studies involved the outbursting magnetic binary Z CMa (Szeifert et al. 2010), the Herbig Ae star HD 101412 with resolved magnetically split lines, and HD 31648 = MWC 480 (Hubrig et al. 2010, 2011d).

Spectropolarimetric observations of a sample of 21 Herbig Ae/Be stars observed with FORS 1 have been used to search for a link between the presence of a magnetic field and

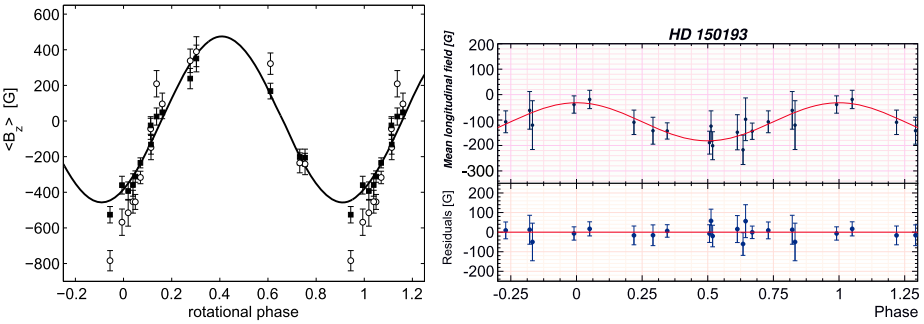

Fig. 6 *Left panel*: Phase diagram of HD 101412 with the best sinusoidal fit for the net longitudinal magnetic-field measurements using all lines (*filled squares*) and hydrogen lines (*open circles*). *Right panel*: Phase diagram of HD 150193 with the best sinusoidal fit for $\langle B_z \rangle$ using all lines. The residuals (observed–calculated) are shown in the lower panel

other stellar properties (Hubrig et al. 2009c). This study did not indicate any correlation of the strength of the net longitudinal magnetic field with disk orientation, disk geometry, or the presence of a companion. No simple dependence on the mass-accretion rate was found, but the range of observed-field values qualitatively supported the expectations from magnetospheric accretion models with dipole-like field geometries. Both the magnetic field strength and the X-ray emission showed hints of a decline with age in the range of $\sim$ 2–14 Myr probed by the sample, supporting a dynamo mechanism that decays with age. Furthermore, the stars seemed to obey the universal power-law relation between magnetic flux and X-ray luminosity established for the Sun and main-sequence active dwarf stars.

A series of net longitudinal magnetic-field measurements was recently obtained at low resolution with the multimode instrument FORS 2 at the Very Large Telescope (VLT) for the Herbig Ae/Be stars HD 97048, HD 101412, HD 150193, and HD 176386 (Hubrig et al. 2011a). Magnetic fields of the order of $\langle B_z \rangle = 120$–$250$ G were for the first time detected in these stars a few years ago during a visitor run with FORS 1 in May 2008 (Hubrig et al. 2009b). In these observations, Herbig Ae/Be stars exhibit a single-wave variation in $\langle B_z \rangle$ during the stellar rotation cycle. This behavior is usually considered as evidence of a dominant dipolar contribution to the magnetic-field topology. Presently, the Herbig Ae star HD 101412 possesses the strongest net-longitudinal magnetic field ever measured in any Herbig Ae star, with a surface magnetic field $\langle B_z \rangle$ up to 3.5 kG (Wade et al. 2005, 2007). HD 101412 is also the only Herbig Ae/Be star for which the rotational Doppler effect was found to be small in comparison to the magnetic splitting, and several spectral lines observed in unpolarized light at high dispersion are resolved into magnetically split components (Hubrig et al. 2010, 2011a).

To date, magnetic-field geometries have been studied for the two SB2 systems HD 200775 (B3 primary) and V380 Ori (B9 primary) (Alecian et al. 2008, 2009), and presumably single stars HD 101412, HD 97048, HD 150193, and HD 176386 (Hubrig et al. 2010, 2011a). As an example, phase diagrams of the magnetic data for the Herbig Ae/Be stars HD 101412 and HD 150193 folded with the determined magnetic/rotation periods are presented in Fig. 6.

The magnetic-field model for the Herbig Ae star HD 101412 is described by a centered dipole with a polar magnetic-field strength B_d between 1.5 and 2 kG and an inclination of the magnetic axis to the rotation axis β of $84 \pm 13^\circ$ (Hubrig et al. 2011d). The fact that the dipole axis is located close to the stellar equatorial plane is very intriguing in view of the generally assumed magnetospheric accretion scenario that magnetic fields channel the

accretion flows towards the stellar surface along magnetic field lines. As was shown in the past (Romanova et al. 2003), the topology of the channeled accretion critically depends on the tilt angle between the rotation and the magnetic axis. For large inclination angles β, many polar field lines would thread the inner region of the disk, while the closed lines cross the path of the disk matter, causing strong magnetic braking, which could explain the observed unusually long rotation period of HD 101412 of about 42 days.

Since about 70 % of Herbig Ae/Be stars appear in binary/multiple systems (Baines et al. 2006), special care must be taken in assigning the measured magnetic field to the particular component in the Herbig Ae/Be system. Alecian et al. (2008) reported on the discovery of a dipolar magnetic field in the Herbig Be star HD 200775, which is a double-lined spectroscopic binary system. However, the magnetic field was discovered not in the component possessing a circumstellar disk and dominating the Hα emission; thus the evolutionary status of the primary B3 component is unclear yet (Benisty et al. 2013). Similar to the case of HD 200775, the frequently mentioned discovery of a magnetic field in the Herbig SB2 system HD 72106 (Alecian et al. 2009) refers to the detection only in the primary component, which is a young main-sequence star, but not in the Herbig Ae secondary (Folsom et al. 2008). The same uncertainty in the evolutionary status applies to the magnetic field detection in the system V380 Ori reported by Alecian et al. (2009). The authors report on the presence of a dipole magnetic field of polar strength 2.12 ± 0.15 kG on the surface of the chemically peculiar primary V380 Ori system. V380 Ori has spectral type around B9 and has been observed in great detail over many wavelength ranges (e.g., Hamann and Persson 1992; Rossi et al. 1999; Stelzer et al. 2006). It has a close infrared companion, with a separation of $0.15''$ at PA 204° (Leinert et al. 1997). Alecian et al. (2009) found that the primary in the V380 Ori system is itself a spectroscopic binary with a period of 104 days, with the secondary being a massive T Tauri star. More recently, Reipurth et al. (2013) report that V380 Ori is a hierarchical quadruple system with a fourth component at a distance of $8.8''$ and position angle 120.4°. Since no periodicity was found in the behavior of the emissions in hydrogen, helium, calcium, and oxygen lines (the lines determining the Herbig Ae/Be nature), it is possible that the primary chemically peculiar component with the detected-dipolar magnetic field is already in advanced age, and the Herbig Be status of the primary is merely based on the appearance of emission in the above-mentioned lines belonging to the secondary T Tauri component.

The presence of a magnetic field on the surface of the Herbig Ae star HD 190073 has been known for several years. The first measurement of a net longitudinal magnetic field in HD 190073 was published by Hubrig et al. (2009c), indicating that $\langle B_z \rangle = 84 \pm 30$ G measured on FORS 1 low-resolution spectra at the 2.8σ level. Catala et al. (2007) then observed this star using the ESPaDOnS spectrograph mounted on the Canada-France-Hawaii Telescope (CFHT) and confirmed the presence of a weak magnetic field, $\langle B_z \rangle = 74 \pm 10$ G, at a higher significance level. A few years later Hubrig et al. (2009c) reported $\langle B_z \rangle = 104 \pm 19$ G using FORS 1 measurements. The measurement of the net longitudinal magnetic field using the available archival HARPS observations from May 2011, $\langle B_z \rangle = 91 \pm 18$ G, presented in this work fully confirms the presence of a rather stable weak field. Surprisingly, new observations of this star during July 2011 and October 2012 by Alecian et al. (2013) detected variations of the Zeeman signature in the LSD spectra on time scales of days to weeks.

The authors suggest that the detected variations of Zeeman signatures are the result of the interaction between the fossil field and the ignition of a dynamo field generated in the newly born convective core. Careful spectropolarimetric monitoring over the next years will be important to confirm the reported variability of the magnetic field. Furthermore, since HD 190073 is very likely a binary system (Baines et al. 2006), special care must be taken in the interpretation of magnetic-field measurements.

As mentioned above, all previously studied Herbig Ae/Be stars exhibit a single-wave variation in the net longitudinal magnetic field during the stellar rotation cycle. These observations are usually considered as evidence for a dominant dipolar contribution to the magnetic field topology. Magnetospheric accretion theories traditionally consider that simple ∼kG dipolar magnetic fields truncate the disk and force in-falling gas to flow along the field lines. The assumption of dominant dipolar fields is usually made for simplicity or because of the lack of available information about the true large-scale magnetic field topology of these stars. Indeed, the recent work of Adams and Gregory (2012) shows that high-order field components may even play a dominant role in the physics of the gas inflow, as the accretion columns approach the star.

The rather new diagnostic He I λ 1.083 μm emission line is considered as probing inflow (accretion) and outflow (winds) in the star-disk interaction region of accreting T Tauri and Herbig Ae/Be stars. The uniqueness of this probe derives from the metastability of this transition and makes it a good indicator of wind and funnel flow geometry (Edwards et al. 2006). Furthermore, according to Edwards et al., the He I line appears in emission for stronger mass-accretion rates and in net absorption for low mass-accretion rates. Modeling of this line allowed Gregory et al. (in preparation) for the first time to study the influence of field topologies on the star-disk interaction. Their models use magnetic fields with an observed degree of complexity, as determined via field extrapolation from stellar magnetic maps.

In Fig. 7, one can find recent high-resolution CRyogenic high-resolution Infrared Echelle Spectrograph (CRIRES) observations of the spectral regions containing the He I λ 1.083 μm line and the hydrogen recombination line Paγ at 1.094 μm over the rotation period of HD 101412 (Hubrig et al. 2012a). The rather strong variation of the line profile of the He I line indicates that the magnetic field of this star is likely more complex than a dipole field. Variable behavior of the He I λ 1.083 μm line was also discovered in a recent X-shooter spectra of the magnetic Herbig Ae stars HD 190073 and PDS 2 (see Fig. 8).

Knowledge of the magnetic-field strength and topology is indispensable for understanding the magnetospheres of Herbig Ae/Be stars and their interaction with the circumstellar environment consisting of a combination of disk, wind, accretion, and jets. Progress in understanding the disk-magnetosphere interaction can, however, only come from studying a sufficient number of targets in detail to look for various patterns encompassing this type of pre-main sequence stars.

Before concluding this topic, we call attention to the work of Bagnulo et al. (2012) and Landstreet et al. (2014), who have questioned the credibility of previous detections of weak magnetic fields at the 3–4σ level with the FORS1 instrument on the ESO VLT. They find that consistency checks among different observations of the same star reveal external errors that are at least 30–40 % larger than can be explained by the cited photon statistics and that alternative reduction procedures provide significantly different (and often smaller) values for the mean longitudinal fields. They suggest that small instrument flexures and velocity shifts and "occasional outliers" likely limit the ability of FORS1 to obtain reliable fields weaker than 100–200 G. Bagnulo et al. (2012) argued that many of the published detections of weaker fields are spurious and not confirmed by measurements with high-resolution spectropolarimeters such as ESPaDOnS (Silvester et al. 2009), but that stronger field measurements by FORS1, for example many Ap/Bp stars, are generally confirmed (Landstreet et al. 2014).

Bagnulo et al. (2012) found that of the five Herbig Be stars that Hubrig et al. (2009c) cites as new detections with errors of 3.4–4.5σ, four (PDS2, HD 100546, HD 135344B, and HD 176386) appear to be spurious and two (HD 97048 and HD 150193) are possible

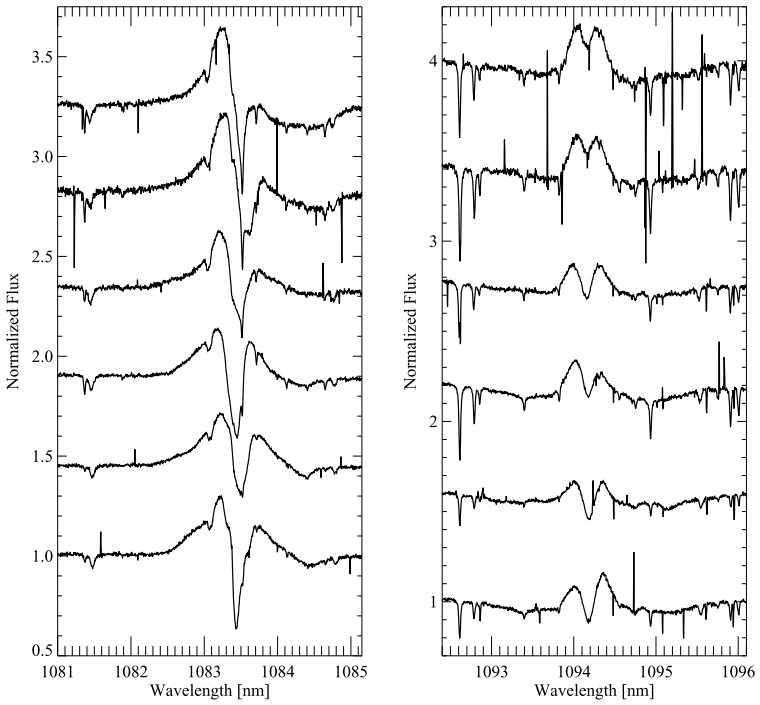

Fig. 7 Recent observations of HD 101412 with the CRyogenic high-resolution Infrared Echelle Spectrograph (CRIRES). *Left panel*: The variability of the He I λ 1.083 μm line profile over the rotation period. Obviously, the field of HD 101412 appears more complex than just a dipole. *Right panel*: Variations of the hydrogen recombination line Paγ at 1.094 μm at the same rotation phases. The Paγ line at 1.094 μm is frequently employed for calculating the mass accretion rate in the way presented by Gatti et al. (2008)

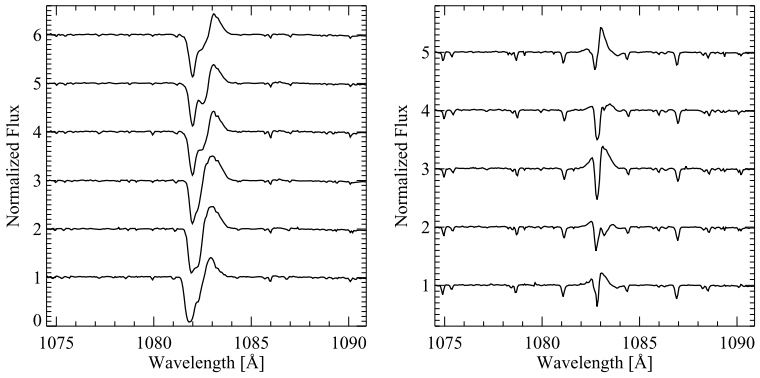

Fig. 8 Recent X-shooter observations of the He I λ 1.083 μm line profile in the magnetic Herbig Ae stars HD 190073 (*left panel*) and PDS 2 (*right panel*) at different epochs. The spectra are shifted vertically for clarity

detections. In subsequent observations with FORS2, Hubrig et al. (2011d) found weak sinusoidally varying fields in HD 97048, HD 150193, and HD 176386, but the cited errors are in the 3–4σ range. At present, the identification of magnetic fields in a few Herbig Be

stars (e.g., HD 76106B, HD 101412 and HD 190073) are confirmed, weak fields appear to be present but are not definitely established in several stars, but most Herbig Be stars do not have detected magnetic fields.

5 Main Sequence Stars

5.1 Low Mass Stars

The very small values of the surface-averaged net longitudinal component of the solar magnetic field are a consequence of the almost complete cancellation of the spectropolarimetric signal by oppositely oriented magnetic fields. Similar measurements for nearby bright G and K stars like ξ Boo A and 61 Cyg A also show weak magnetic fields of 10–30 Gauss and 13 Gauss, respectively (Plachinda and Tarasova 2000; Plachinda et al. 2001). One must conclude that the typical morphology of late-type dwarf stars is highly complex, and, therefore, different observing techniques are required to understand the magnetic-field strengths and morphologies of these stars.

5.1.1 Zeeman Broadening Observations

Robinson et al. (1980) first showed that measurements of Zeeman broadening of spectral lines in unpolarized light can be used to measure the mean magnetic-field strength $\langle B \rangle = B_{\rm MOD} f$ averaged over the surface of a late-type star. This technique described in Sect. 2 has been applied to a number of mostly active stars (see tables in Reiners 2012), but the technique has its limitations as described in detail by Anderson et al. (2010) and Saar (1988).

Anderson et al. (2010) analyzed high-resolution optical spectra of four stars with spectral types similar to the Sun, two slowly rotating quiet stars, 61 Vir (G6 V) and the Sun (G2 V) viewed as a star by reflected light from Ganymede, and two rapidly rotating active stars, 59 Vir (G0 V) and HD 68456 (F6 V). They computed spectral line profiles by radiative transfer calculations in local thermodynamic equilibrium (LTE) model atmospheres with a range of broadening parameters to best fit the observed line profiles. These calculations were for both single-component and two-component model atmospheres for which one component could be hotter (plage region), the same, or cooler (starspot) than the mean temperature structure. They found that $\langle B \rangle$ is consistent with zero for the two quiet stars, 600–1200 Gauss for HD 68456, and about 500 Gauss for 59 Vir. However, they identified a number of systematic effects (e.g., line blends, overly simplified treatment of turbulence, and LTE atmospheres) and concluded that a more fruitful approach would be to analyze Zeeman broadening of infrared spectral lines with large Landé g values, because then Zeeman broadening is much larger than the other broadening mechanisms.

An early example of applying the near-infrared Zeeman-broadening technique to measure magnetic fields was the study of the active star ϵ Eri (K2 V) and two other K stars (40 Eri and σ Dra) by Valenti et al. (1995). They observed the Fe I 1.56485 μm line with Landé $g = 3.0$ and 15 other nearby Fe I lines with smaller g factors. By modelling the Fe I line profiles with marginally resolved σ components, they were able to measure separately the unsigned magnetic-field modulus $B_{\rm MOD} = 1.44 \pm 0.2$ kG and filling factor $f = 0.088 \pm 0.025$. The corresponding value of $B_{\rm MOD} f = 0.13$ kG. With the same technique, Johns-Krull and Valenti (1996) modelled the Fe I 8468.4 Å line with Landé $g = 2.5$ in four M dwarfs. Figure 9 shows the significant Zeeman broadening of the Fe I lines of the two active stars, EV Lac (M4.5e) and GJ 729 (M4.5e), relative to less active comparison

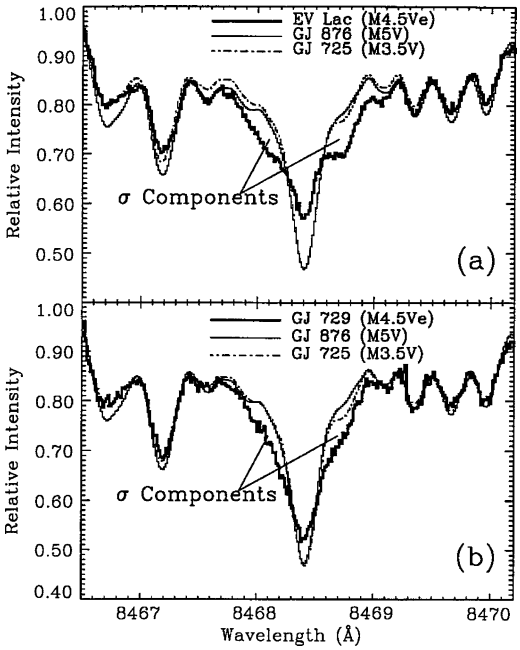

Fig. 9 Comparison of Stokes I spectra of the Fe I 8468.40 Å line of two active M dwarfs (EV Lac and GJ 729) compared to less active stars. This comparison demonstrates that the excess line broadening for the two active stars is magnetic rather than blending by TiO lines, which should be the same for all of these stars. Figure from Johns-Krull and Valenti (1996)

stars that the authors identify as the splitting of the σ components of the stellar magnetic fields. Since this splitting is larger than other broadening mechanisms, their spectral synthesis analysis determined the mean magnetic fields and filling factors separately rather than as the product of $B_{\rm MOD} f$. They found $B_{\rm MOD} = 3.8 \pm 0.5$ kG and $f = 0.50 \pm 0.13$ for EV Lac and $B_{\rm MOD} = 2.6 \pm 0.3$ kG and $f = 0.5 \pm 0.13$ for Gl 729. These magnetic field strengths are larger than the maximum field strengths seen in solar active regions and likely result from the higher pressure in M dwarf photospheres and the balance between magnetic pressure ($B^2/8\pi$) in magnetic flux tubes and gas pressure in the nonmagnetic photosphere.

Figure 10 shows that for G–M dwarfs, the observed magnetic-field strengths are approximately equal to the equipartition field set by pressure balance between the magnetic pressure in flux tubes and the nonmagnetic-photospheric gas pressure outside of the flux tubes. This pressure balance is also seen in solar active regions (plages) but not in sunspots, where the emergent spectrum is depressed to higher pressure layers below the normal photosphere. T Tauri stars show the same effect, although the reason is not yet clear. This figure also shows that f increases with rotation period according to the relation $f = 79$–$64 \log(P)$. Cuntz et al. (1999) have used a similar relation in computing a two-component (nonmagnetic and magnetic flux tube) model chromosphere for ϵ Eri. This relation probably does not contain significant bias resulting from the different rotation rates or activity of the magnetic star and the comparison low activity star, because the widths of low Landé g spectral lines in the active and inactive stars have the same shape whereas the shapes of the high Landé g lines differ greatly and show marginally or completely resolved sigma components for the active star.

Reiners and Basri (2007, 2010) and Shulyak et al. (2011) have extended this study of M dwarf magnetic fields to include more than 80 stars in the spectral range M2.0 to M9.5 by fitting the Zeeman-broadened lines of molecular FeH near 1.0 μm. The average magnetic-field strengths of these stars range up to $\langle B \rangle = 4$ kG (see Fig. 11) with a large range at each spectral type. Except for the coolest stars in their sample (spectral types M7 to M9.5),

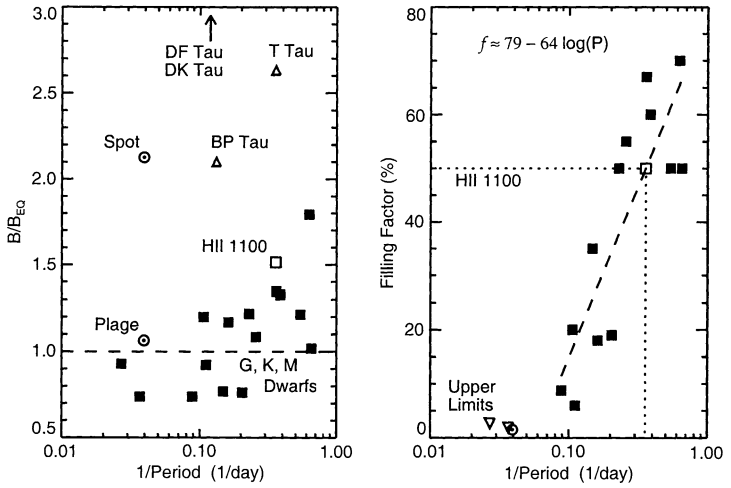

Fig. 10 (*left*) Ratio of the measured-unsigned magnetic-field modulus to the equipartition magnetic field strength when the magnetic pressure ($B^2_{\rm MOD}/8\pi$) equals the photospheric gas pressure. The *dashed-horizontal line* corresponds to measured-magnetic fields equal to the equipartition field. *Triangles* indicate T Tauri stars and ⊙ symbols refer to solar features (plage and sunspot). (*right*) Filling factors ($100 \times f$) vs. rotational periods for G–M dwarf stars. Figure from Valenti and Johns-Krull (2001)

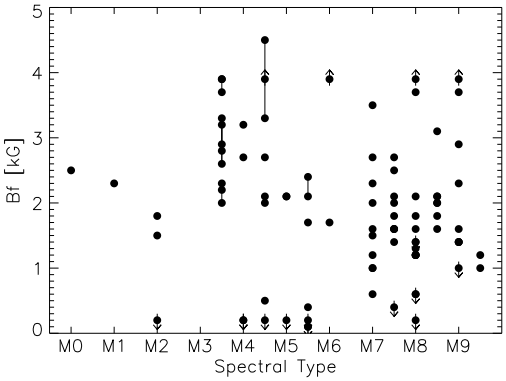

Fig. 11 A summary of mean-unsigned magnetic-field strengths $\langle B \rangle = B_{\rm MOD} f$ of M dwarf stars obtained mostly with the Zeeman-broadening technique (Reiners 2012). For stars at each spectral type, there is a wide range in Bf, but a maximum value near 4000 G

the magnetic field strength increases with rotational velocity, as is seen in G and K stars. Although these measurements could not separate $B_{\rm MOD}$ from f, many of these stars have $B_{\rm MOD} f \approx 4$ kG, similar to EV Lac, for which $f = 0.50 \pm 0.13$ (Johns-Krull and Valenti 1996). This summary suggests that for the active cool M dwarfs, about half of the stellar photosphere has magnetic fields as strong as $B_{\rm MOD} \approx 8$ kG.

The Ti I spectral lines near 2.2 μm, which provide even larger Zeeman splittings, are useful for measuring magnetic-field strengths and filling factors of M dwarfs like AD Leo (Saar and Linsky 1985). The combination of large Zeeman splitting and high signal/noise Ti I spectra of the T Tauri star TW Hya (see Sect. 4.1) permitted Valenti and Johns-Krull (2001) to determine the distribution of magnetic-field strengths and corresponding filling factors across the stellar surface.

The measured values of $B_{\rm MOD} f$ are correlated with the commonly used indicators of magnetic activity and heating. Figure 12 shows the correlation of $B_{\rm MOD} f$ with the Rossby

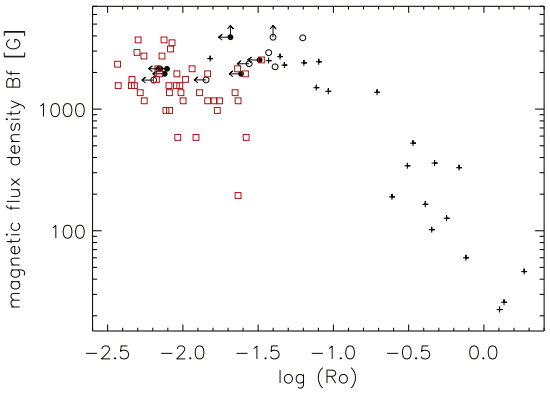

Fig. 12 Correlation of the mean-unsigned magnetic-field strength, $B_{\mathrm{MOD}} f$, with Rossby number R_0. Crosses are solar-type stars, and circles are M0–M6 stars. *Red squares* are M7–M9 stars. These data show a rotation-activity relation for slowly rotating stars (large R_0) and saturation for rapidly rotating stars (small R_0). Figure from Reiners (2012)

number, $R_0 = P_{\mathrm{rot}}/\tau_{\mathrm{conv}}$, where P_{rot} is the stellar rotational period, and τ_{conv} is the convective turnover time, which is not a well-defined theoretical quantity. It is usually computed empirically as the mass-dependent convective turnover time that minimizes scatter in the rotation-activity relation as described by Reiners (2012). "R_0 is an important parameter for the dynamo generation of magnetic fields. Figure 12 shows the log-log rotation-activity relation for slower-rotating stars and saturation for the faster-rotating stars. The ratio of Hα luminosity to bolometric luminosity, log $[L_{\mathrm{H}\alpha}/L_{\mathrm{bol}}]$ vs. log R_0 shows the same type of correlation (Reiners 2012).

5.1.2 Zeeman Doppler Imaging

Doppler imaging produces a brightness map of a stellar surface by inverting a time sequence of high-resolution spectra that contain the brightness and Doppler shift of absorption lines produced in each spatial resolution element on the stellar surface (Vogt and Penrod 1983). Although such inversions have many solutions, several regularization techniques lead to robust solutions of the two-dimensional brightness maps. Zeeman-Doppler imaging is the extension of the DI procedure with polarizing optics, as first proposed by Semel (1989) and developed by Donati and Brown (1997). The first applications of ZDI to stars used only circular polarization data (Stokes V), but recent developments in instrumentation and polarized radiative-transfer calculations (Piskunov and Kochukhov 2002) allow the analysis of both circular- and linear-polarized spectra (Stokes IVQU). Donati and Landstreet (2009) provide a comprehensive review of this topic.

ZDI works because the longitudinal and transverse components of the vector magnetic field produce different Zeeman patterns as a function of velocity when the magnetic vector is viewed from the advancing limb to the star's central meridian and then to the receding limb. The circular polarization Zeeman patterns (net after cancellation) are different for the radial, azimuthal (toroidal), and meridional components of the magnetic field, as shown in Fig. 13. Linear-polarization Zeeman patterns show different center-to-limb effects for the radial, azimuthal, and meridional magnetic fields. Since high signal-to-noise data are required to detect weak circular and especially linear polarization, Donati and Brown (1997) pioneered the use of a very large number of spectral lines to create ZDI images.

Before describing some of the major accomplishments of ZDI, we should mention the limitations of the technique. First, and most important, ZDI measures the large-scale net magnetic-field strength and not the unsigned magnetic-field strength because the circular and linear polarization data are net values after cancellation by oppositely oriented fields in

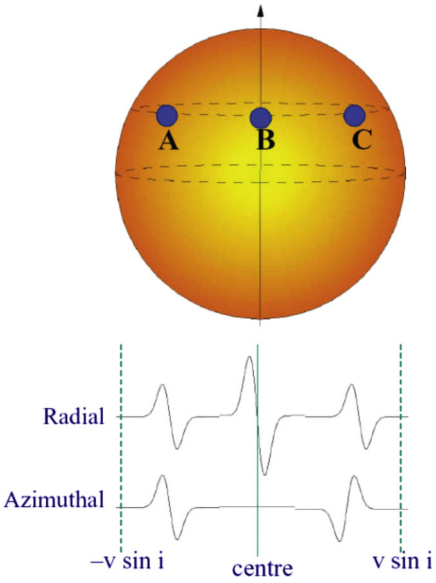

Fig. 13 A schematic representation of the circular-polarization Zeeman spectrum (V/I) of an absorption line formed in a magnetic field. If the magnetic field is radial relative to the star (and therefore longitudinal at disk center as viewed by an observer), the Zeeman pattern is strongest on the stellar meridian and retains the same symmetry, but weakens, as the radial field is observed towards the stellar limbs. If the magnetic field is azimuthal (E–W direction) relative to the star (and therefore transverse at disk center and longitudinal at the limbs), the Zeeman pattern is strongest at the limbs (but opposite symmetry) and zero at disk center. If the magnetic field is in the meridional direction (N–S direction, not shown in the figure), the Zeeman pattern is observed only toward the poles. Figure from Hussain (2004)

each spatial resolution element. Also important are the effects of irregular or large gaps in the time spacing, uncertainty in the inclination of the star's rotation axis relative to the line of sight, possible crosstalk between the Stokes parameters, line blends, different temperatures (and thus continuum brightness) of magnetic compared to nonmagnetic regions, evolution of the stellar magnetic topology during the multiday observing sequence, and poorly understood instrumental and systematic errors. Despite these limitations, ZDI studies have found that the topologies of active G–M stars, which are younger and likely precursers of older stars like the Sun, differ considerably from what we know about the Sun in the following ways:

Importance of Azimuthal Fields ZDI images of active solar-mass stars typically show strong azimuthal fields that are not seen in inactive stars like the Sun. A good example is the study by Morgenthaler et al. (2012) of the magnetic field on ξ Boo A, a G8 V star rotating almost four times faster than the Sun ($P_{\rm rot} = 6.43$ days). As shown in Fig. 14, the reconstructed net magnetic field includes a strong azimuthal component that contains most of the net magnetic field in the 2007 and 2011 data sets when Ca II emission indicated that the star was most active. For solar-mass stars, the magnetic energy in large-scale fields increases with the rotation rate (Vidotto et al. 2014): most of this magnetic energy is in the poloidal field for slow rotators like the Sun, but the fraction stored in azimuthal fields increases with rotation rate and dominates the poloidal fields when $P_{\rm rot} \leq 12$ days (Petit et al. 2008; see Fig. 15). ZDI images of the very rapidly rotating ($P_{\rm rot} = 0.51479$ days)

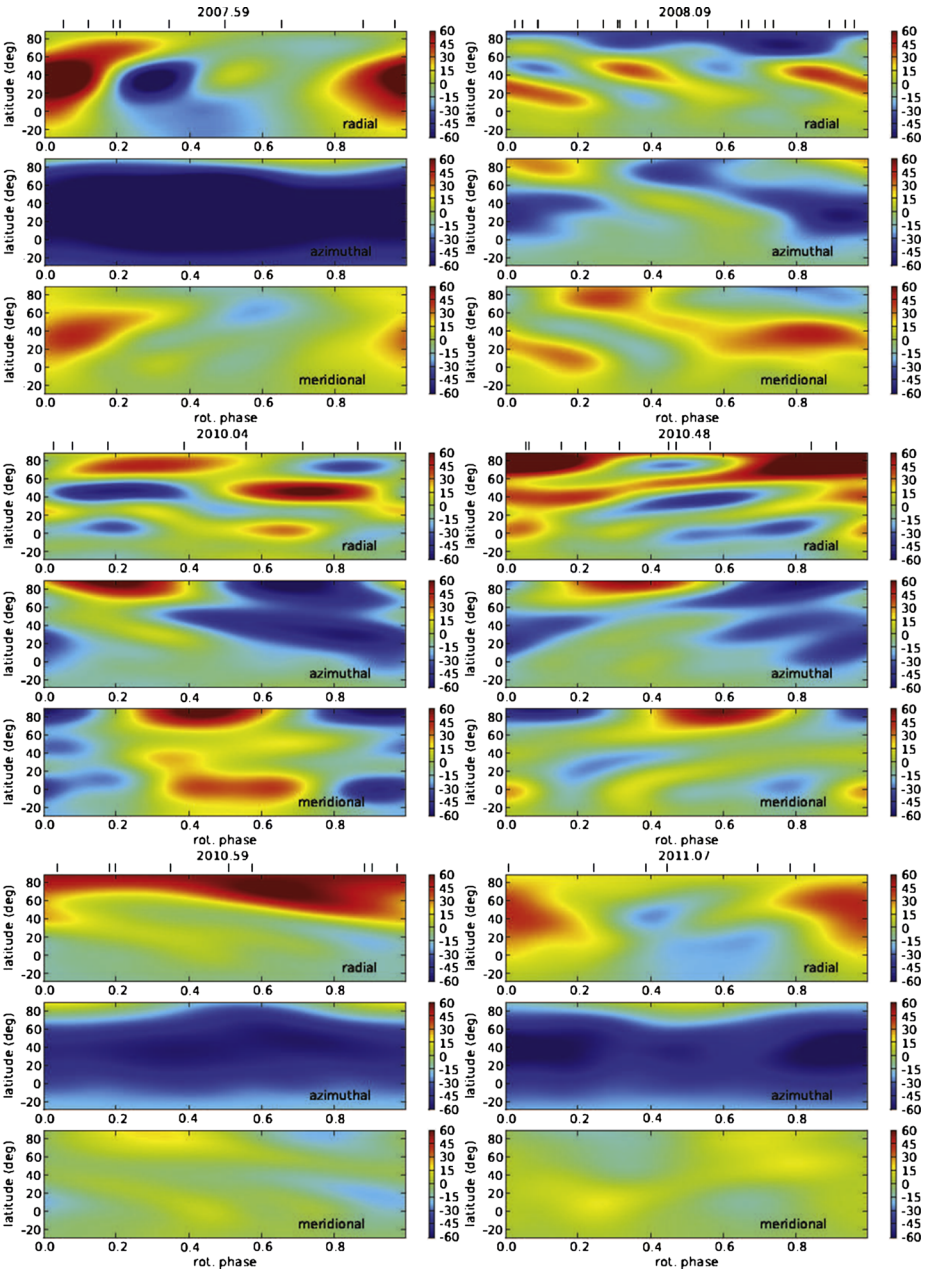

Fig. 14 Reconstructed net magnetic-field maps of ξ Boo A for the radial, azimuthal,and meridional components obtained at five times between 2007 and 2011 by Morgenthaler et al. (2012). The strong azimuthal component contains the most of the magnetic energy when the star is most active (2007 and 2011)

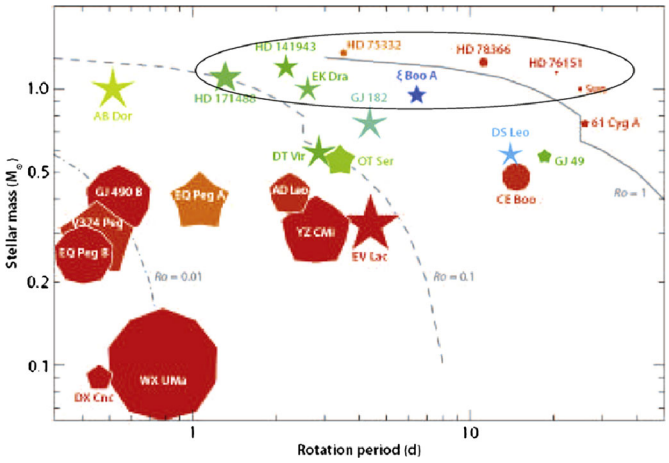

Fig. 15 A summary of the large-scale magnetic topologies and fluxes obtained from ZDI images as a function of stellar mass, rotation period, and Rossby number (R_0). Symbol size indicates the relative magnetic energy density, and symbol color indicates field topology with blue for purely toroidal and red for purely poloidal fields. The symbol shape indicates the degree of asymmetry (decagon for purely axisymmetric poloidal fields and stars for purely nonaxisymmetric poloidal fields). The encircled area contains the Sun and more rapidly rotating solar-mass stars. Figure adapted from Donati and Landstreet (2009)

young K0 V star AB Dor show strong azimuthal fields both at high latitude (70°–80°), which appears to encircle a polar spot, and at intermediate latitudes with opposite sign (Donati et al. 1999; Hussain et al. 2002). The net magnetic field in these azimuthal fields exceeds 1 kG in some places with the high latitude azimuthal flux the largest measured flux on this star.

Relation of Net Magnetic Fields to Unsigned Field Strengths The net magnetic fields for ξ Boo A shown in Fig. 14 would suggest that $B_{\rm NET} = 30 - 100$ G if one assumes that $f = 1.0$ and no field cancellation. This result should be compared to the measurements of the spatially resolved solar magnetic-field modulus, $B_{\rm MOD} \approx 1600$ G. The value of $B_{\rm MOD}$ for ξ Boo A should be similar to, or somewhat larger than, solar as the star is slightly cooler than the Sun with higher photospheric gas pressure and, therefore, higher equipartition magnetic-field strength. Zeeman-broadening measurements of ξ Boo A lie in the range $\langle B \rangle = B_{\rm MOD} f = 0.34 - 0.48$ kG (Reiners 2012). Marcy and Basri (1989) measured $\langle B \rangle = 0.35$ kG with $B_{\rm MOD} = 1600$ G, similar to the Sun, and $f = 0.22$. If one assumes this value for the filling factor, the observed net magnetic field is 30–100 G corresponds to $B_{\rm NET} = 140$–450 G, which can be compared to the resolved field strength $B_{\rm MOD} = 1600$ G. Since the magnetic energy density is proportional to $B^2_{\rm MOD}$, field cancellation means that the ZDI image only represents 1–10 % of the photospheric magnetic energy of this star. Other ZDI images likely also represent only a small fraction of the magnetic energy in a stellar photosphere. Lang et al. (2014) estimate the amount of small-scale flux not found in ZDIs of M stars and extrapolate the small-scale and large-scale photospheric fields into the stellar coronae.

Dependence on Age and Rotation Vidotto et al. (2014) find that for non-accreting main-sequence stars in the unsaturated regime, that is stars older than 10^7 years, magnetic fields decay with increasing age and rotation period $P_{\rm rot}$. They find this decay to be the case for both $\langle B \rangle$, measured from Stokes I spectra, and for an unsigned version of $\langle B_z \rangle$, measured

from ZDI images. The power-law dependencies are similar, $\langle B \rangle \propto P_{\rm rot}^{-1.7}$ and unsigned $\langle B_z \rangle \propto P_{\rm rot}^{-1.32\pm0.14}$, respectively, indicating that the large-scale fields, measured from ZDI images, and the small-scale fields, measured from Zeeman broadening and splitting spectra, are coupled (Vidotto et al. 2014). These authors suggest that the same dynamo field-generation processes are responsible for both the small-scale and large-scale fields.

Large-Scale Magnetic Morphology of Early and Late M Dwarfs In a series of papers, Donati et al. (2008a) and Morin et al. (2008, 2010) obtained ZDI images of 23 M dwarf stars to study whether the magnetic topologies of M dwarfs are different for stars with radiative cores and presumably solar-like $\alpha\Omega$-type dynamos ($M > 0.35\ M_\odot$) compared to stars that are fully convective with different types of dynamo processes ($M < 0.35\ M_\odot$). One finding is that for stars with similar parameters (i.e., similar Rossby numbers), there are two very different magnetic topologies (strong dipolar and weaker multipolar) that may indicate a bistability with two possible dynamo states or an age effect (cf. Gastine et al. 2013; Vidotto et al. 2014). Despite this topological diversity, many of the more massive M dwarfs ($M > 0.5\ M_\odot$) have strong azimuthal fields and weak poloidal fields, but with decreasing mass, axisymmetric poloidal fields dominate over the toroidal fields and produce stronger large-scale magnetic fluxes, as shown in Fig. 15. The strong azimuthal fields seen in the more massive M dwarfs, which have radiative cores, are also seen in the young classical T Tauri stars (see Sect. 4.1), which are fully convective. Why these two star types with very different interior structures have similar magnetic topologies has not been explained and may provide an important clue concerning magnetic dynamos.

There is evidence for evolution of the reconstructed magnetic topologies for the less massive stars on time scales of less than one year. The fully convective stars likely have a higher degree of large-scale field organization as the ratio of net magnetic-field strength measured in the circular polarization data to the unsigned magnetic-field strength inferred from the magnetic-broadening data is only about 15 % for these stars compared to only a few percent for the more massive stars with radiative cores. The more massive M stars, like the G and K stars, have complex fields on small spatial scales.

Variable Magnetic Topology ZDI images of the solar-type star HD 190771, which rotates nearly three times faster than the Sun ($P_{\rm rot} = 8.8$ days), show large changes in the magnetic morphology in the course of one year (2007 to 2008; Petit et al. 2009). These changes include polarity reversal in the axisymmetric and azimuthal fields and a sharp decrease in the magnetic energy stored in the azimuthal component.

Nonpotential Magnetic Fields and Large Magnetic Loops Hussain et al. (2002) showed that the magnetic field of the very rapidly rotating star AB Dor contains about 20 % nonpotential energy in the photosphere and about 14 % nonpotential energy in the corona. This nonpotential energy indicates strong electric currents in both locations, which is very different from the slowly rotating Sun. Also, sequences of high-resolution spectra provide evidence for large slingshot-type prominences anchored at high latitudes that are probably magnetic loops extending outward to several stellar radii that co-rotate with the photosphere.

5.2 The Chemically Peculiar Stars

Spectra of chemically peculiar (CP) main-sequence A- and B-type stars contain abnormally strong or weak absorption lines of certain elements (e.g., Si, Sr, Cr, Eu, or He). These stars generally have magnetic fields that can be detected through circular-polarization observations of spectral lines. Observables, such as the magnitudes in various photometric bands,

Table 2 Different groups of chemically peculiar stars

Peculiarity type	Spectral type	$T_{\rm eff}$ range	Magnetic	Spots
He-strong	B1-B4	17 000–21 000	yes	yes
He-weak	B4-B8	13 000–17 000	yes	yes
Si	B7-A0	9000–14 000	yes	yes
HgMn	B8-A0	10 000–14 000	yes?	yes!
SrCrEu	A0-F0	7000–10 000	yes	yes
Am	A0-F0	7000–10 000	yes?	no

spectral line equivalent widths, and magnetic-field properties, vary with the same period, which can range from half a day to several decades. Abnormal line strengths correspond to element overabundances (by up to 5–6 dex with respect to the Sun) in the stellar outer layers. The CP star class is roughly represented by three subclasses: the magnetic Ap and Bp stars, the metallic-line Am stars, and the HgMn stars. An overview of the different groups of CP stars can be found in Table 2. Indirect evidence for kG magnetic fields in these stars consists of strong gyrosynchrotron emission detected at cm wavelengths (Linsky et al. 1992) and an X-ray flare seen in the A0p star IQ Aur (Robrade and Schmitt 2011). About a few percent of intermediate-mass main-sequence stars are identified as Ap/Bp stars (Landstreet et al. 2007; Donati and Landstreet 2009).

The first detection of the net-longitudinal magnetic field in a star other than the Sun was achieved in CS Vir by Babcock in 1946 (Babcock 1947). Today, net-longitudinal magnetic-field measurements throughout the variation period have been obtained for no more than 100 stars. The resolution of magnetically split lines requires a sufficiently strong magnetic field and slow rotation. Resolved magnetically split lines were first discovered in Babcock's star, HD 215441 (Babcock 1960), for which he measured a net magnetic-field modulus of $B_{\rm MOD} \sim 34$ kG, which is the strongest magnetic-field modulus measured in an Ap star to date. However, Elkin et al. (2010) found that the Ap star HD 75049 with $B_{\rm MOD} \sim 28$ kG (see Fig. 16) is a close rival to Babcock's star, Hubrig et al. (2005) found that the cool Ap star HD 154708 has $B_{\rm MOD} \sim 24.5$ kG, and Kochukhov et al. (2011) showed that the He-strong star HD 37776 may have an even stronger surface magnetic field. In 1987, 12 stars with magnetically resolved lines were known, but only four of those were studied throughout their variation period. By 2001, 44 stars with magnetically resolved lines were known, with 24 of those were studied throughout their variation period (Mathys et al. 1997; in preparation). The first systematic determinations of the crossover effect and the mean quadratic magnetic field were published in 1995 by Mathys (1995a, 1995b). A full phase coverage was achieved for about two dozen stars. The bulk of the published material on broad-band linear polarization (BBLP) was gathered by Leroy between 1990 and 1995 (Leroy 1995, and references therein). Variations in BBLP are well studied for about 15 stars.

As shown in Fig. 17, the strongest magnetic fields tend to be found in more massive stars, but also in fast-rotating stars (Hubrig et al. 2000). All CP stars with rotation periods exceeding 1000 days have magnetic fields below 6.5 kG. However, a great many Ap stars have short periods typically 2–4 days (Hubrig et al. 2000). From the finding that the net-longitudinal magnetic field averaged over the stellar disk is not zero, one can directly conclude that the magnetic field must be organized on a larger scale, either as a dipole or a superposition of a dipole and a quadrupole. The circular polarization from tangled, solar-like magnetic fields mostly cancels out in a disk integration. The magnetic field of Ap stars

thus has a significant dipole-like component. For a dipole, the ratio between the longitudinal magnetic field and the magnetic-field modulus $\langle B_z \rangle / B_{\rm NET}$ is 0.3, for a quadrupole it is 0.05. If toroidal or higher-order multipolar components were sufficient to account for the observed net-longitudinal magnetic field, these components would induce strong distortions of the spectral line profiles in Stokes I, i.e., in integral light, which is not seen.

The magnetic field covers the whole CP stellar surface homogeneously, i.e., the distribution of the field strength over the star is fairly narrow. Evidence for this distribution comes from the fact that the magnetic field is observed at all phases, the continuum is reached between the split components of resolved lines, and that the resolved magnetically split components are rather narrow (Mathys et al. 1997).

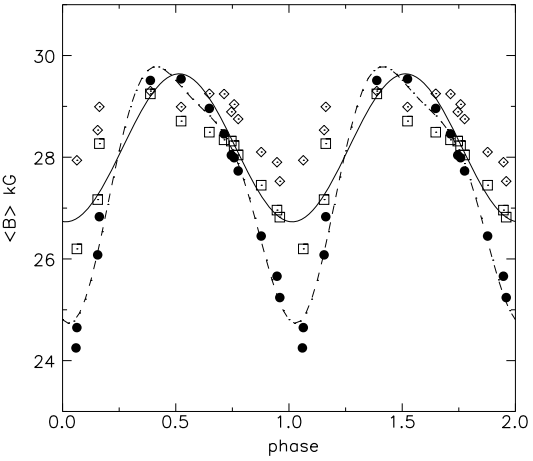

Fig. 16 Variation of the magnetic field modulus of HD 75049 with rotational phase. Different symbols refer to measurements using different ions. The *solid line* is the fit to the data obtained using the hydrogen lines, and the *dashed line* is the fit using the FeII lines. Figure from Elkin et al. (2010)

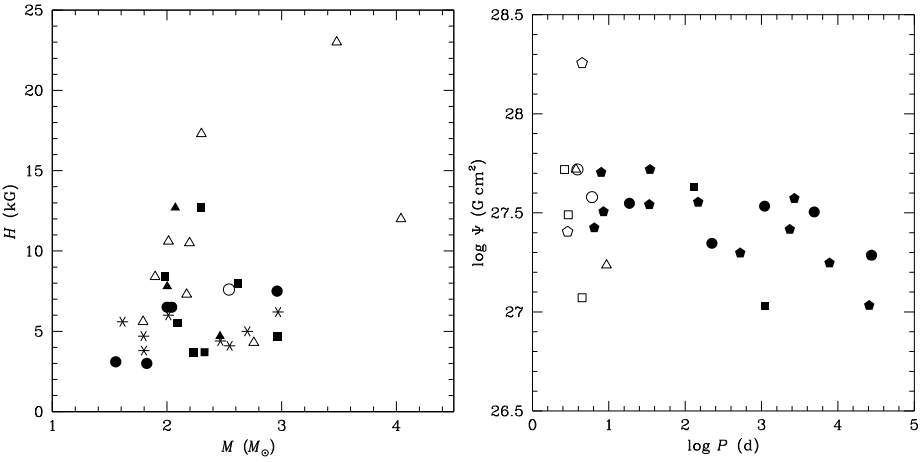

Fig. 17 *Left*: Plot of the mean magnetic field modulus as a function of stellar mass for Ap stars. Triangles are for stars with $P_{\rm rot} \leq 10$ days, squares for periods 10–1000 days, and asterisks for periods longer than 1000 days. *Right*: Plot of magnetic flux as a function of rotational period for Ap stars. Filled symbols are for stars with magnetically-resolved spectral lines. Open symbols are for stars for which mean quadratic fields are available. Figures are from Hubrig et al. (2000)

Magnetic fields have severe effects on the structure of stellar outer layers. They are responsible for magnetically controlled winds and elemental-abundance stratification. Evidence for abnormal atmospheric structure comes from the profiles of hydrogen Balmer lines in cool Ap stars that cannot be fitted by conventional models. This structure has also a potential impact on the net-longitudinal magnetic-field determination by Balmer-line polarimetry. The core-wing anomaly (Cowley et al. 2001) of the hydrogen Balmer lines leads to the impossibility of fitting the Balmer lines with one temperature. For example, to fit the Hβ line in HD 965, one needs to assume $T_{\rm eff} = 5500$ K for the core of the line and $T_{\rm eff} = 7000$ K for the wings.

The magnetic field is not symmetric with respect to the stellar rotation axis. Other surface features, e.g., the abundance distribution, are determined by the magnetic field. Since the observed variations result from changing aspects of the visible hemisphere as the star rotates, the variation period must be the rotation period of the star. No intrinsic variations of the magnetic field have been observed in Ap stars over time scales of decades.

In early models of the magnetic field, a quasi-sinusoidal variation of the longitudinal magnetic field was assumed. In the simplest model, a dipole centered at the star's center and with an axis inclined with respect to the stellar rotation axis, was employed. Stars with magnetically resolved lines show that the magnetic-field modulus generally has one maximum and one minimum per rotation period, even for stars with a reversing-longitudinal magnetic field (Mathys et al. 1997) (see Fig. 16). From these observations, a centered dipole can be ruled out. Alternative models include a dipole that is offset along its axis (parameters: i, β, $B_{\rm d}$, a), or a collinear dipole plus a quadrupole (parameters: i, β, $B_{\rm d}$, $B_{\rm q}$), with i the inclination angle of the star with respect to the line of sight, β the inclination angle of the magnetic field with respect to i, $B_{\rm d}$ the strength of the dipole, $B_{\rm q}$ the strength of the quadrupole, and a the offset of the dipole with respect to the star's center. The models must make a good match with four observables: the maximum and the minimum of both the longitudinal magnetic field and the magnetic-field modulus. Both classes of models are equivalent to first order.

Additional constraints on the magnetic field geometry can come from the crossover and the mean-quadratic magnetic field. A collinear dipole plus a quadrupole and an octupole give good first approximations in many cases (Landstreet and Mathys 2000). The dipole primarily accounts for the longitudinal magnetic field, the quadrupole gives the field strength contrast between the poles, and the octupole is responsible for the equator-to-pole field strength contrast. Asymmetric variation curves can be determined from some magnetic-field moments. They exist when the magnetic field is not symmetric about an axis passing through the center of the star (Mathys 1993) and can be described with a generalized-multipolar model (Bagnulo et al. 2000, and references therein). The input observables for these models are all available observables of the magnetic field: $\langle B_{\rm z}\rangle$, $\langle x B_{\rm z}\rangle$, $\sqrt{\langle B^2\rangle + \langle B_{\rm z}^2\rangle}$, $\langle B_{\rm NET}\rangle$, and the BBLP, where x is the stellar equatorial velocity times the sine of the inclination angle. Landolfi et al. (1998) has shown that the inversion of these measured quantities provide information on the strength and orientations of the dipole and quadrupole components of the stellar magnetic field subject to the limitations imposed by measurement errors. In particular, the quantity $\sqrt{\langle B^2\rangle + \langle B_{\rm z}^2\rangle}$ is needed to determine the presence and properties of the quadrupole component of the magnetic field. A χ^2 minimization between the predicted and observed values of the observables at phases distributed throughout the rotation period will determine the final model for the geometric structure of the magnetic field.

Ultimately, a direct inversion of the line profiles recorded in all four Stokes parameters will allow one to derive magnetic-field maps without a-priori assumptions. Since inversion is an ill-posed problem, a regularization condition is needed. This condition is achieved with

the Zeeman Doppler-imaging technique (ZDI) (Piskunov and Kochukhov 2002). It is very demanding in terms of the signal-to-noise ratio in the data, spectral resolution, and phase coverage. So far, these inversions are restricted to a few individual stars (e.g., Kochukhov et al. 2004; Lüftinger et al. 2010; Kochukhov and Wade 2010; Silvester et al. 2012; Rusomarov et al. 2013). Inversion of the phase-resolved full Stokes IVQU spectrophotometric data set for the A0pSiEuHg star α^2CVn revealed a global dipolar-like topology with localized spots of higher field intensity (Kochukhov and Wade 2010). Recent magnetic-field maps of α^2 CVn obtained by Silvester et al. (2014b, 2014a) confirm the complex substructure of the magnetic field and show that low-order multipole models fail to match the observed maps. They also find that the magnetic-field topology of this star has been stable for the last 10 years and that maps based on strong absorption lines tend to smooth the finer scale structure seen in maps constructed from weak absorption lines. The chemical abundance enhancements are correlated with the radial magnetic field in patterns that are not predicted by theoretical models. In particular, some elements (e.g., O, Cl, and Eu) are enhanced in areas with negative radial magnetic fields, whereas other elements (e.g., Fe, Cr, Si, Ti, and Nd) are deleted where the magnetic fields are weak but overabundant where $B_{\rm MOD} \sim 2$ kG, irrespective of sign.

The magnetic-field modulus much better characterizes the intrinsic-stellar magnetic field than the net-longitudinal magnetic field, which is much more dependent on the geometry of the observation. Most Ap stars with magnetically resolved lines have a magnetic-field modulus (averaged over the stellar rotation period) between 3 and 9 kG, but there is a lower cutoff of the distribution at 2.8 kG, (Landstreet et al. 2007; Aurière et al. 2007), which corresponds to the thermal equipartition fields in the photospheres of Ap and Bp stars (Donati and Landstreet 2009). For Ap stars with masses greater than 3 $M\odot$, the magnetic-field strenghs decline rapidly with age, but the lower mass Ap stars do not show this behavior (Landstreet et al. 2007). One should be able to resolve lines down to 1.7 kG or lower at some rotation phases of some stars, but only for one target is the resolution sufficient to observe down to 2.2 kG. The lower limit of the magnetic-field distribution is roughly temperature independent; hotter stars may have stronger magnetic fields than cooler stars (Mathys et al. 1997).

Ap star variation periods span five orders of magnitude. Until recently, there appeared to be no systematic differences between short- and long-period stars. A confirmation that very long periods are indeed rotation periods has been brought by BBLP (Leroy et al. 1994). The systematic study of 40 Ap stars with resolved magnetically split lines has doubled the number of known Ap stars with $P > 30$ days (Mathys et al. 1997). The distribution of periods longer than 1 year is compatible with a uniform distribution on a logarithmic scale. No star with $P > 150$ d has a magnetic-field modulus exceeding 7.5 kG. More than 50 % of the Ap stars with resolved lines and shorter periods have a magnetic-field modulus above this value (Mathys et al. 1997). In the collinear dipole plus quadrupole and octupole model, the angle between the magnetic and rotation axes β is generally smaller than 20° for stars with $P > 30$ d, unlike short period magnetic Ap stars for which this angle is usually large (Landstreet and Mathys 2000).

HgMn stars are chemically peculiar stars with spectral type B8 to A0 and $T_{\rm eff} =$ 10 000–14 000 K. They show extreme overabundance of Hg (up to 6 dex) and/or Mn (up to 3 dex). They display the most obvious departures from abundances expected within the context of nucleosynthesis (Cowley and Aikman 1975). More than 150 HgMn stars are known, many of which are found in young associations (Sco-Cen, Orion OB1). They are among the most slowly rotating stars on the upper main sequence and have exceptionally stable atmospheres with an average rotational velocity of $\langle v \sin i \rangle = 29$ km/s, which leads to extremely sharp-lined spectra. They are the best-suited targets to study isotopic and hyperfine structure. More than 2/3 of the HgMn stars belong to spectroscopic binary (SB) systems with a

prevalence of $P_{\rm orb} \approx 3$–20 d, and many HgMn stars are in multiple systems. The spectrum variability seen in HgMn stars is due to the presence of chemical spots. These stars do not have strong large-scale organized magnetic fields, but tangled magnetic fields are possible. They do not have enhanced strengths of rare earth elements but rather of the heavy elements W, Re, Os, Ir, Pt, Au, Hg, Tl, Pb, and Bi, which makes these stars natural laboratories for the study of heavy elements. They also show anomalous isotopic abundances for the elements He, Hg, Pt, Tl, Pb, and Ca.

One of the most exciting objects containing a HgMn star is the triple system AR Aur. The inner two stars constitute the only known eclipsing binary including a HgMn star. This binary has an orbital period of 4.13 d and an age of 4 Myr. The two stars are of spectral types B9V and B9.5V, and while the primary HgMn star is exactly on the zero-age main sequence (ZAMS), the secondary is still contracting (e.g., Nordstrom and Johansen 1994). Hubrig et al. (2012b) used observations with SOFIN high-resolution optical spectrograph at the Nordic Optical Telescope to study the distribution of different elements over the surface of the primary HgMn star using the Doppler-mapping technique. From the same data set, they also measured a weak longitudinal magnetic field in the primary star with 3–4σ errors. AR Aur shows a similar behavior to other HgMn systems discussed by Hubrig et al. (2012b). The results suggest a correlation between the proposed magnetic field, the abundance anomalies, and the binary properties. For the synchronously rotating components of the SB2 system AR Aur, the stellar surfaces facing the companion star usually display low-abundance element spots and negative magnetic-field polarity. The surface of the opposite hemisphere, as a rule, is covered by high-abundance element spots and the putative magnetic field is positive at the rotation phases of the best-spot visibility (Hubrig et al. 2012b). Since the reanalysis of the FORS1 data that Hubrig et al. (2006b) used to identify weak longitudinal fields in four HgMn stars did not confirm the presence of fields in these stars (Bagnulo et al. 2012) and Kochukhov et al. (2013) found no evidence for tangled magnetic fields in any HgMn stars, the present conclusion is that these stars do not have measured magnetic fields.

The He-strong early B stars are the most massive and hottest of the chemically peculiar stars. They are very rapid rotators; the most rapidly rotating star in this class, HR 7355, has a rotational period of 0.52 days, about 90 % of critical. Rivinius et al. (2013) showed that this star's magnetic-field topology is more complex than an oblique dipole and that the magnetic poles are the regions with the strongest He overabundances and the lowest metal overabundances. The B2Vp star σ Ori E shares many of the same properties as HR 7355 with a similar magnetic-field topology and chemical abundances at the magnetic poles, but with a slower rotational period (1.19 days) and higher $T_{\rm eff}$ (Oksala et al. 2012). For a third member of the He-strong subgroup, HD 37776, ZDI shows a very complex magnetic field with a magnetic-field modulus, $B_{\rm MOD} = 43$–49 kG, depending on the assumed topology, that could be stronger than for Babcock's star (Kochukhov et al. 2011). The magnetic field appears to contain a toroidal component.

5.3 Pulsating B Stars

β Cep stars are short-period (3–8 h) pulsating variables of spectral type O9 to B3 (corresponding to a mass range of 8–20 $M_\odot$) along the main sequence that pulsate in low-order pressure (p) and/or gravity (g) modes. Slowly pulsating B (SPB) stars show variability with periods of the order of 1 d, are less massive (3–9 $M_\odot$) main sequence B-type stars, and have multiperiodic high-order low-degree g mode oscillations.

A long-term monitoring project aimed at asteroseismology of a large sample of SPB and β Cep stars was started by researchers of the Institute of Astronomy of the University of

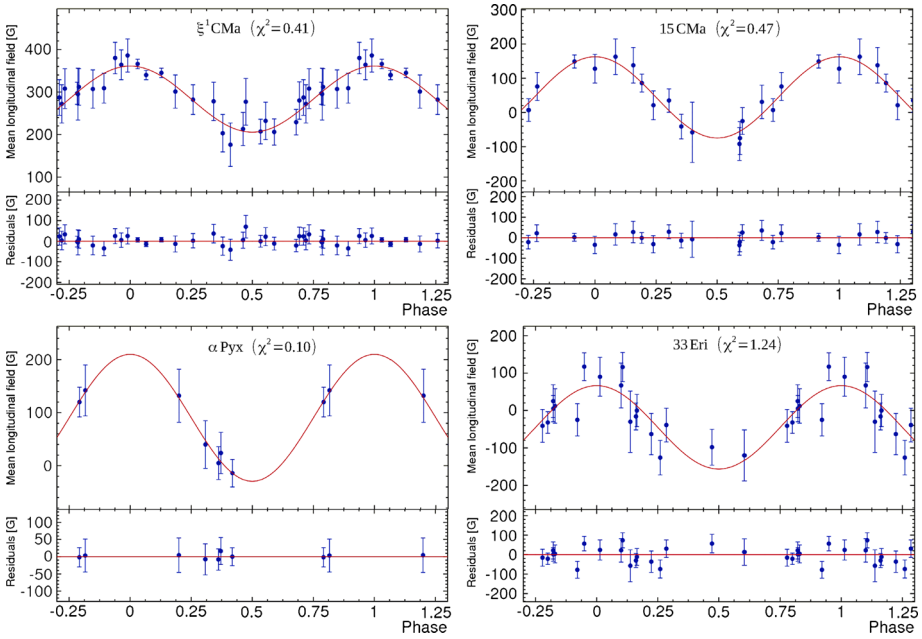

Fig. 18 Phase diagrams with the best sinusoidal fit for the net longitudinal magnetic-field strength measurements. The residuals (observed–calculated) are shown in the lower panels. The deviations are mostly of the same order as the error bars; no systematic trends are obvious, which justifies a single sinusoid as a fit function

Leuven more than 10 years ago. In the first publication on a magnetic survey of pulsating B-type stars with FORS 1, Hubrig et al. (2006a) announced detections of weak net-longitudinal magnetic fields of a few hundred Gauss in a number of SPB stars and in the β Cep star ξ^1 CMa, whose field of the order of 300–400 G is one of the largest among all currently known magnetic β Cep stars. Bagnulo et al. (2012) has confirmed the detection of two of the SPB stars (HD 53921 = V450 Car and HD 208057 = 16 Peg) and listed two others as possible detections (HD 74195 = o Vel and HD 152511 = V847 Ara). Reanalysis of the data for one or a few observations of the other SPD stars did not confirm the earlier detections of weak longitudinal magnetic fields. In the continuation of their FORS1 observing program, Hubrig et al. (2009a) listed six β Cephei stars and 18 SPB stars as having magnetic fields at the $\geq 3\sigma$ level, but Bagnulo et al. (2012) was able to confirm only one of the β Cephei stars (HD136504 = ϵ Lup) and none of the individual observations of the other SPB stars. The β Cephei star ξ^1 CMa (HD 46328), however, is a confirmed detection with a strong magnetic field $\langle B_z \rangle = 338 \pm 11$ G (Silvester et al. 2009, 2012). HD 180642 = V1449 Aql is another β Cephei stars with a strong longitudinal magnetic field and a dipolar field of about 3 kG. The differences between FORS1 detections (Hubrig et al. 2006b, 2009a) and the nondetections based on a alternative reductions of the same data by Bagnulo et al. (2012) are discussed at the end of Sect. 4.2.

In Fig. 18, one can see the results of magnetic-field monitoring of four β Cep and SPB stars. Although many of the individual measurements of the stars shown in the figure are not significant at the 3σ level, the plots of longitudinal magnetic fields phased with the rotational period reveal patterns that can be simply explained by oblique rotator models. From FORS 1/2 and the higher resolution SOFIN observations, Hubrig et al. (2011c) determined

Table 3 Measurements of the mean longitudinal magnetic field using high-resolution HARPS spectra

Object	MJD	S/N	$\langle B_z \rangle$
HD 74195	55605.217	220	-70 ± 21
HD 74195	55606.130	300	-14 ± 18
HD 74560	55605.221	240	56 ± 19
HD 74560	55606.134	280	8 ± 18
HD 74560	55607.177	350	-35 ± 15
HD 85953	55600.305	230	79 ± 20

a rotation period of $P = 2.1795$ d for ξ^1 CMa, which is nearly a factor of two smaller than found by Fourtune-Ravard et al. (2011), who determined $P \sim 4.2680$ d from ESPaDOnS observations. Note that in the latter work, the impact of pulsations on the magnetic-field measurements from high-resolution spectra was not taken into account. The effects of not including pulsations in the analysis of low-resolution FORS1 spectra can be large but not readily quantifiable (Hubrig et al. 2011e), whereas pulsation effects on high-resolution Stokes V data may not be large (Silvester et al. 2012).

Among the sample of SPB stars with detected magnetic fields using FORS 1, three stars, HD 74195, HD 74560, and HD 85953, have been observed in February 2011 with the high-resolution ($R = 115,000$) polarimeter HARPSpol, installed at the European Southern Observatory (ESO) 3.6 m telescope on La Silla, in the framework of the guaranteed-time observer (GTO) program 086.D-0240(A). The star HD 85953 was observed once, whereas HD 74195 was observed on two different nights, and HD 74560 was observed on three different nights. Additional spectra were downloaded from the ESO archive and reduced using the HARPS data reduction software available at the ESO headquarters in Germany. For the measurements of the magnetic fields, the moment technique developed by Mathys (e.g., Mathys 1991) was used. Formally significant detections above the 3σ level were achieved in HD 85953 and in one observation of HD 74195 (see Table 3; Hubrig et al., in preparation). In line with the discoveries of weak magnetic fields in pulsating stars, Briquet et al. (2013) found a magnetic field in the hybrid SPB/β Cep star HD 43317.

The pulsation amplitudes for the three-studied pulsating stars range from 4.5 to 25 mmag. The study of correlations between the strength of magnetic fields and pulsational characteristics (Hubrig et al. 2009b) indicates that it is possible that stronger magnetic fields appear in stars with lower-pulsating frequencies and smaller-pulsating amplitudes. Spectra for all three sources can be found in Fig. 19. Spectral variability is evident for the two objects with more than one observation.

From the FEROS (Fiber-fed Extended Range Optical Spectrograph) time series, one can find line profile variability for V1449 Aql with a pulsating frequency of $f_{\rm puls} = 5.487$ d^{-1}. The variability in the spectra of V1449 Aql and the impact of pulsations on the polarimetric spectra can be seen in Fig. 20. Neglecting the rapid changes in the line profiles shapes due to pulsations in the analysis of spectropolarimetric data can lead to nondetections of magnetic fields in these stars (Hubrig et al. 2011e) or even spurious magnetic detections (Schneer et al. 2006). The need for a careful observing procedure is especially important for large amplitude pulsators like V1449 Aql (Hubrig et al. 2011e).

5.4 Be Stars

Rapidly rotating Be stars lose mass and initially accumulate it in a rotating circumstellar disk. Much of the mass loss is in the form of outbursts, and thus additional mechanisms,

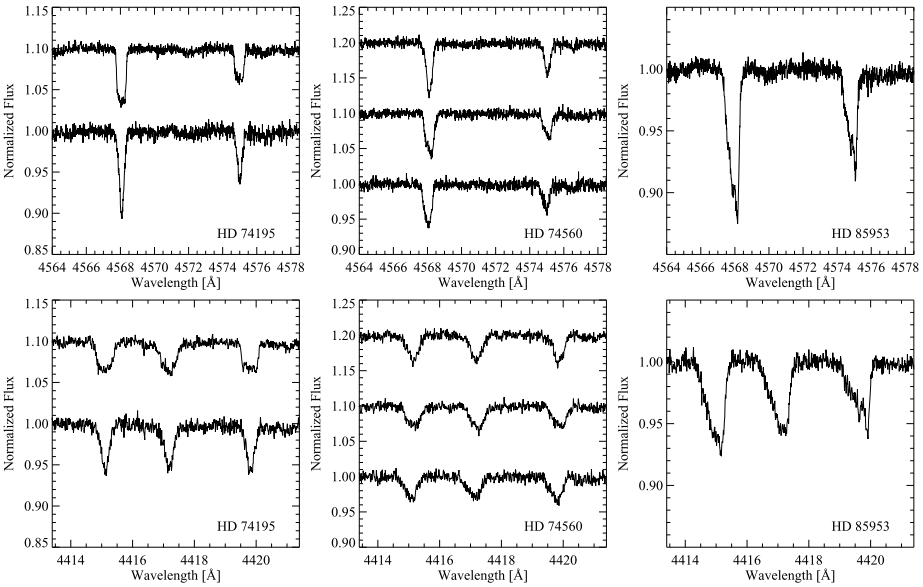

Fig. 19 Spectral variability as seen in HARPS Stokes I spectra. *Left*: HD 74195, *middle*: HD 74560, *right*: HD 85953

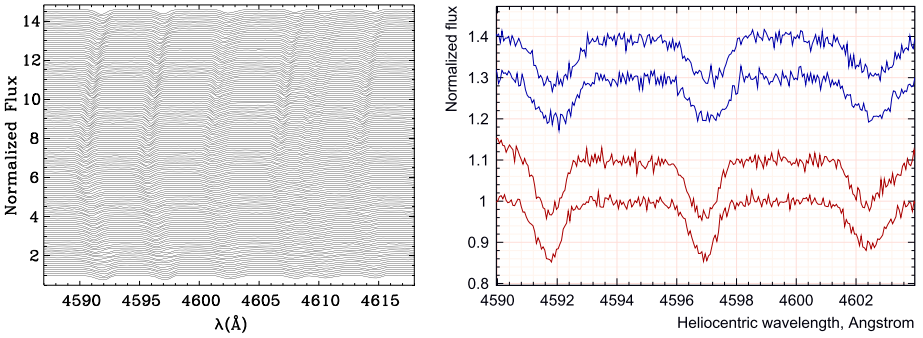

Fig. 20 *Left*: Time series of FEROS (Fiber-fed Extended Range Optical Spectrograph) spectra for V1449 Aql showing pulsational line-profile variability in the spectral region 4590–4615 Å. The pulsation phase zero is at the bottom. *Right*: Variability of the output spectra in two SOFIN subexposures taken with the quarter-wave plate angles separated by 90° taken around HJD 2455398.530. The lower two spectra, $(I+V)_0$ and $(I-V)_0$, correspond to the first subexposure, while the upper spectra, $(I-V)_{90}$ and $(I+V)_{90}$, correspond to the second subexposure. The strong effect of pulsations on the line-profile shapes and the line positions is clearly visible between the spectra of the first subexposure with a duration of 20 min and the spectra of the second subexposure with the same duration

such as the beating of nonradial pulsation modes or magnetic flares, must be at work. Indirect evidence for the presence of a magnetic field are variations of X-ray emission and transient features in absorption line profiles. Angular momentum transfer to a circumstellar disk, channeling stellar wind matter, and accumulation of material in an equatorial disk are more easily explained if magnetic fields can be invoked. Fifteen Be stars have been observed with the hydrogen polarimeter by Barker et al. (1985) using Hβ, but no magnetic fields were

detected. One Be star with a reported magnetic field, ω Ori (Neiner et al. 2003), was not confirmed as magnetic by recent observations.

A sample of Be stars in the field and in the cluster NGC 3766 (14.5–25 Myr old) was observed by Hubrig et al. (2009b) in 2006–2008 with FORS 1. A few Be stars show weak magnetic fields with the strongest field detected in HD 62367 ($\langle B_z \rangle = 117 \pm 38$ G, $m_V = 7.1$). Usually, the detected magnetic fields are below 100 G (see Figs. 21 and 22). Since the magnetic fields are weak, it is difficult to determine their large-scale structure. The cluster NGC 3766 appears to be extremely interesting, where evidence can be found for the presence of a magnetic field in seven early-B type stars (among them three Be stars) out of the observed 14 cluster members (Hubrig et al. 2009a).

For nine early-type Be stars, the authors obtained time-resolved magnetic-field measurements over ∼one hour (up to 30 measurements) with FORS 1 at the VLT. For λ Eri, they were able to detect a period of $P = 21.1$ min in the magnetic-field measurements (see Fig. 23). The spectral line profiles of λ Eri exhibit short-time periodic variability (see Fig. 24) because of non-radial pulsations with a period of 0.7 d (Kambe et al. 1993b). Fur-

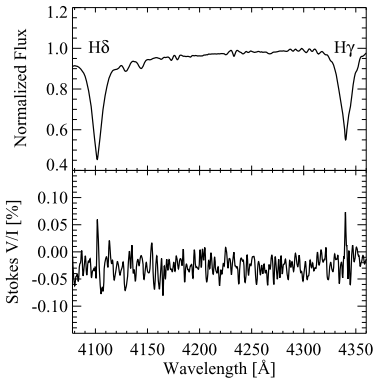

Fig. 21 Stokes I and Stokes V spectra of the Be star o Aqr ($\langle B_z \rangle = 98 \pm 31$ G) in the region including the Hδ and Hγ lines

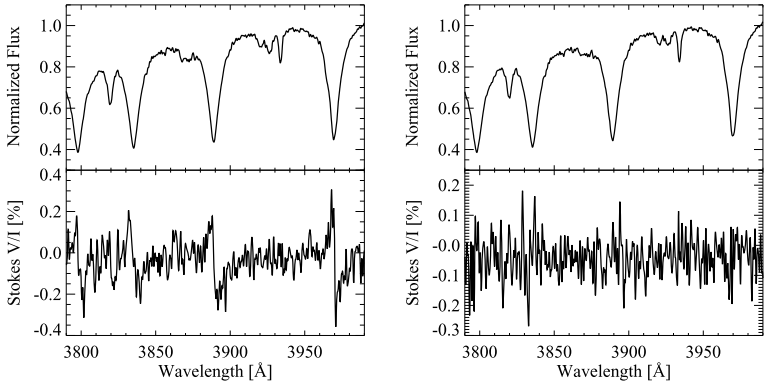

Fig. 22 *Left*: Stokes I and Stokes V spectra in the blue spectral region around high-number Balmer lines of the He peculiar member NGC 3766-170 of the young open cluster NGC 3766 with the magnetic field $\langle B_z \rangle = 1559 \pm 38$ G measured on hydrogen lines. *Right*: Stokes I and Stokes V spectra around high-number Balmer lines for the candidate Be star NGC 3766-45, with a net-longitudinal magnetic field $\langle B_z \rangle = -194 \pm 62$ G measured on hydrogen lines

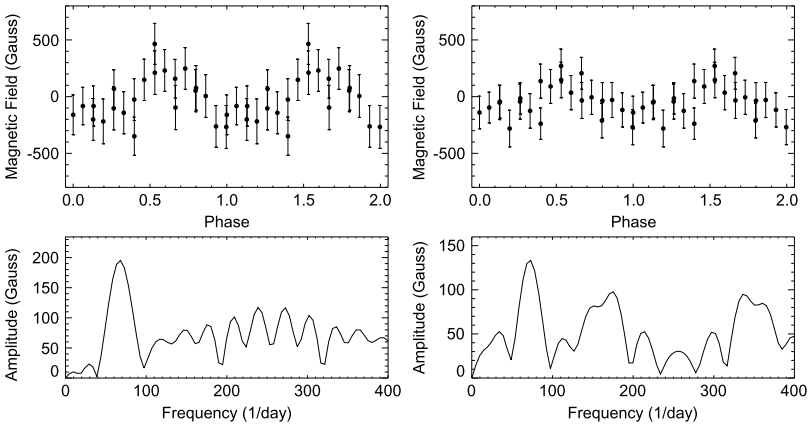

Fig. 23 Phase diagram and amplitude spectrum for the net-longitudinal magnetic-field strengths of λ Eri in 2006 August using hydrogen lines (*left*) and all lines (*right*)

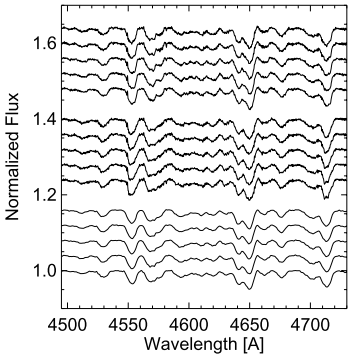

Fig. 24 Spectrum variability of λ Eri on three different nights: on 2006 August 8 (*bottom*), 2007 November 27 (*middle*), and 2007 November 28 (*top*)

thermore, Smith (1994) detected dimples with a duration of 2–4 h. Are these strong local magnetic fields?

Apart from λ Eri, four other stars showed indications of magnetic-cyclic variability on the scales of tens of minutes (Hubrig et al. 2009a). A similar magnetic-field periodicity ($P = 8.8$ min) was detected for the B0 star θ Car (Hubrig et al. 2008b). These stars are good candidates for future time-resolved magnetic-field observations with high-resolution spectropolarimeters.

5.5 OB Stars

The presence of a convective envelope has been assumed to be a necessary condition for significant magnetic activity. Magnetic activity is found all the way from the late A-type stars (e.g., in Altair: Robrade and Schmitt 2009) with very shallow convective envelopes down to the coolest fully convective M-type stars as late as spectral type M9.5 (Reiners and Basri 2007, 2010).

On the other hand, advances in instrumentation over the past decades have led to magnetic-field detections in a small, but gradually growing, subset of massive stars that frequently present cyclic wind variability, Hα emission variations, nonthermal radio/X-ray emission, and transient features in absorption-line profiles.

Magnetic fields have fundamental effects on the evolution of massive stars, their rotation, and on the structure, dynamics, and heating of radiative winds. The origin of the magnetic fields is still under debate: it has been argued that magnetic fields could be "fossil", or magnetic fields may be generated by strong binary interaction, i.e., in stellar mergers, or during a mass transfer or common-envelope evolution.

To identify and model the physical processes responsible for the generation of magnetic fields in massive stars, it is important to understand whether:

- most magnetic stars are slowly rotating,
- magnetic fields appear in stars at a certain age,
- magnetic fields are generated in stars in special environments: Do some clusters contain a larger number of magnetic massive stars, similar to the Ap/Bp content in different clusters (NGC 2516 has the largest number of magnetic Ap stars and X-ray sources)?
- magnetic fields are produced through binary interaction,
- X-ray emission can be used as an indirect indicator for the presence of magnetic fields.

5.5.1 Magnetic Fields in O-type Stars

Early indications of the presence of magnetic fields in O-type stars came from (a) non-thermal radio emission (Beiging et al. 1989; Abbott et al. 1986), indicating gyrosynchrotron emission from energetic electrons in magnetic fields, and (b) X-ray emission in the Fe XXIV and Fe XXV lines (Schulz et al. 2000), indicating plasma as hot as 6.1×10^7 K in the wind of the O7 V star θ^1 Ori C, which is far hotter than predicted by radiation-driven shocks in the stellar wind, The first direct detections of a magnetic field in an O-type star were reported by Donati et al. (2002) for θ^1 Ori C and Donati et al. (2006) for HD 191612. Today, about two dozen magnetic O-type stars are known.

Hubrig et al. (2008a) were the first to determine net-longitudinal magnetic-field strengths for a large sample of O-type stars with an accuracy of a few tens of Gauss, using FORS 1. Very few magnetic fields stronger than 300 G were detected in the studied sample, suggesting that large-scale dipole-like magnetic fields with polar magnetic-field strengths higher than 1 kG are not common among O-type stars. Their studies of massive stars revealed that the presence of a magnetic field can be expected in stars of different classification categories and at different evolutionary stages. No physical properties are known that define particular classes of stars as nonmagnetic. The inability to detect magnetic fields in massive stars in earlier studies could be related to the weakness of these fields, which can, in some stars, be as small as only a few tens of Gauss.

In recent years, two major surveys have been aimed at better understanding the nature and origin of magnetic fields in OB stars and the physics of their atmospheres, winds, and magnetospheres. MiMeS (Wade et al. 2012) focused on high-resolution ($R \approx 65\,000$–$110\,000$) spectropolarimetry with Narval, ESPaDOnS, and HARPS. The BOB consortium (Morel et al. 2014) uses 35.5 nights on FORS 2 and HARPS over a period of 2.5 years. It concentrates on main-sequence OB stars and do not consider, e.g., Be or Wolf-Rayet stars. One half of their targets are early B stars, one third are late O stars, and the rest is made up of several late B stars with only very few early O stars. So far, the BOB consortium has observed of $\sim$100 OB stars, with only very few targets in common with MiMeS. It aims to show consistent detections using different reduction and analysis techniques, independently carried out by two teams.

Overall, the data obtained by various authors seem to confirm that the occurrence of fields above the detectability threshold ($\sim$ 100–200 G) is low in massive stars. An exact estimation of the incidence rate is still pending and may be revised upwards in the future.

While an exact estimate of the incidence rate is still pending, Wade and the MiMeS Collaboration (2014) suggests that about 7 % of Galactic O stars have magnetic fields above this measurement threshold. They strongly suggest that there is a bimodal distribution of O-type stars consisting of a small population of stars with strong (1–3 kG) magnetic fields, generally thought to have an oblique rotator structure, and a much larger population of stars with undetected fields smaller than about 100 G. If confirmed by subsequent measurements, this dicotomy would be an extension to higher mass stars of the "magnetic desert" that Aurière et al. (2007) has proposed for intermediate-mass stars. Citing biases for measuring weak magnetic fields, especially for more rapidly-rotating stars, Fossati et al. (2015) argues that there is no clear evidence for a "magnetic desert" for high mass stars. Recent measurements of magnetic fields on ϵ CMa and β CMa with the high-resolution HARPSpol spectrometer on the VLT now demonstrate the feasibility of obtaining credible longitudinal magnetic fields strengths smaller than 10 G (Fossati et al. 2015) at least for bright stars. New measurements with even better sensitivity are needed to quantify the distribution of magnetic field strengths for OB stars, which is essential for understanding the origin of their magnetic fields and the effects of magnetic fields on the evolution of OB stars. Fortunately, the measurement of weak magnetic fields is helped by magnetic OB stars having, on average, rotation speeds significantly lower than the rest of the OB star population.

A kinematic analysis of known magnetic O-type stars using the best available astrometric, spectroscopic, and photometric data indicates that a magnetic field is more frequently detected in candidate runaway stars than in stars belonging to clusters or associations (Hubrig et al. 2011). The results obtained so far allowed the authors to constrain preliminarily the conditions conducive for the presence of magnetic fields and to derive the first trends for their occurrence rate and field-strength distribution.

To investigate statistically whether magnetic fields in O-type stars are ubiquitous or appear only in stars with a specific spectral classification, certain age, or in a special environment, Hubrig et al. (2011b, 2011) acquired spectro-polarimetric observations with FORS 2. They detected a magnetic field at a significance level of 3σ in eleven stars. The strongest net-longitudinal magnetic fields were measured in two Of?p stars: $\langle B_z \rangle = 381 \pm 122$ G for CPD–28 2561 and $\langle B_z \rangle = 297 \pm 62$ G for HD 148937. Both magnetic fields were detected by them for the first time, the latter in an earlier study (Hubrig et al. 2008a).

Walborn (1973) introduced the class of Of?p stars as the subset of massive O stars that display recurrent spectral variations in certain spectral lines, sharp emission or P Cygni profiles in the He I and Balmer lines, and strong C III emission lines around 4650 Å. Only five Galactic Of?p stars are currently known (HD 108, NGC 1624-2, CPD-28 2561, HD 148937, and HD 191612), and they have all been found to harbor magnetic fields (Martins et al. 2010; Wade et al. 2012a; Hubrig et al. 2011b, 2008a; Donati et al. 2006). Interestingly, a kinematical assessment of space velocities of the three brightest in this class (HD 108, HD 148937, and HD 191612) indicates that all three can be considered as candidate runaway stars (Hubrig et al. 2011b).

The excellent potential of FORS 2 for the detection and investigation of magnetic fields in massive stars is demonstrated in Fig. 25, which shows FORS 2 observations collected between 2008 and May 2011 of the Of?p star HD 148937 together with ESPaDOnS observations obtained at the CFHT (Wade et al. 2012b). The measurement errors for both ESPaDOnS and FORS 1/2 observations are of similar order.

In most magnetic O stars, strong magnetic fields seem to give rise to spectral peculiarities and/or drive periodic line-profile variations (e.g., the Of?p stars or θ^1 Ori C). In contrast, Grunhut et al. (2012) observed a narrow-lined O9.7 V star (HD 54879) hosting an oblique rotator field with a dipole strength of 880 ± 50 G that does not display any evidence for abundance anomalies. Only the broad emission-like Hα profile is variable. This variability may

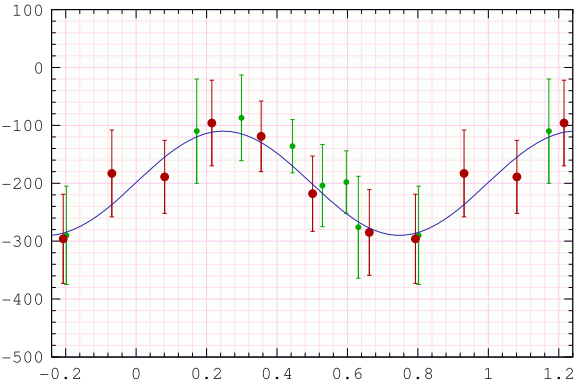

Fig. 25 Net-longitudinal magnetic-field variation of HD 148937 over the 7.032 d period determined by Nazé et al. (2010). *Red* (*large*) symbols correspond to ESPaDOnS observations (Wade et al. 2012b), while *green* (*small*) symbols are FORS 1 and FORS 2 measurements (Hubrig et al. 2008b, 2011b, in preparation)

be related to the presence of a centrifugal magnetosphere where wind material is trapped in closed-magnetic loops and prevented from falling back to the star by centrifugal forces. Petit et al. (2013) classified slowly rotating O-type stars as having dynamical magnetospheres and the more rapidly rotating B-type stars as having centrifugal magnetospheres.

Another interesting discovery is the detection of a magnetic field in a multiple system in the Trifid Nebula (Hubrig et al. 2014), which is a very young and active site of star formation. From observations of the three brightest components (A, C, and D) identified in the central part of this nebula, Kohoutek et al. (1999) clearly detected a circularly polarized signal with FORS2 in component C (HD 164492C). In contrast, no such features were visible for the two other components (an early O star and a Herbig Be star).

The O9.5 V star ζ Ophiuchi is a well-known rapidly rotating runaway star with extremely interesting characteristics. It undergoes episodic mass loss seen as emission in Hα, and it is possible that it rotates at almost break-up speed with $v \sin i = 400$ km s^{-1} (Kambe et al. 1993a). It is probably associated with the pulsar PSR B1929+10. Tetzlaff et al. (2010) suggested that both objects were ejected from Upper Scorpius during the same supernova event. Spectropolarimetric observations of ζ Oph by Hubrig et al. (2011) with FORS 1 in 2008 revealed the presence of a net-longitudinal magnetic field $\langle B_z \rangle_{\rm NET} = 141 \pm 45$ G. Hubrig et al. (2013a) obtained nine additional spectropolarimetric observations with FORS 2 over the rotation period in 2011. The net-longitudinal magnetic field shows a change of polarity, and its variation over the rotation cycle can be represented by a sinusoidal fit with a semiamplitude of ~ 160 G. FORS 2 measurements using all spectral lines can be phased with a period of 1.3 d (Fig. 26). This period is roughly twice the 0.643 d period found from the variation of the He I λ6678 line. MOST (Microvariability and Oscillations of STars) satellite observations discovered a dozen significant oscillation frequencies between 1 and 10 cycles day^{-1} (Walker et al. 2005). The suggested rotation periods using UV and X-ray data range from 0.77 to 0.98 d.

6 Post-Main Sequence Stars

The magnetic-field strengths and topology of post-main sequence stars are very different between rapidly rotating and slowly rotating stars. Subgiant and giant stars can rotate rapidly when members of tidally locked spectroscopic binary systems have orbital periods less than about 20 days, such as the RS CVn systems, or rapid rotators by some other process, such as the FK Com systems. Zeeman-broadening measurements of the primary stars in the

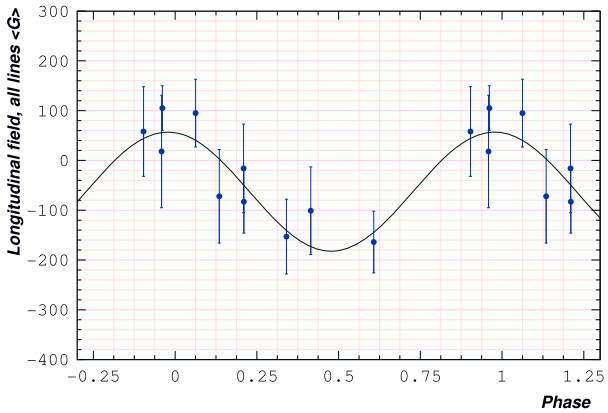

Fig. 26 Phase diagram for the best sinusoidal fit corresponding to the period of 1.3 days for the longitudinal magnetic-field measurements using the whole spectrum for ζ Oph

RS CVn-type systems VY Ari (K3 III–IV) and II Peg (K2–3 IV–V) indicate strong fields with large filling factors. For VY Ari, Bopp et al. (1989) found $B_{\rm MOD} = 2000 \pm 300$ G with $f = 0.66 \pm 0.14$, and for II Peg, Saar (1996) found $B_{\rm MOD} \approx 3000$ G with $f \approx 0.60$

ZDI has provided information on the topology of the magnetic fields of several rapidly rotating giant stars. For example, Petit et al. (2004a) found for HD 199178, an FK Com-type star with $P_{\rm rot} = 3.3$ days, that the radial magnetic flux contains roughly 85 % of the large-scale magnetic energy, but there is also significant azimuthal flux. Comparison with the Zeeman-broadening data for rapidly rotating dwarfs suggests that most of the magnetic energy is in small-scale unresolved magnetic fields. Changes in the magnetic topology are seen on time scales as short as two weeks, and the differential rotation is solar-like, but about 1.5 times faster. Donati et al. (2003) and Petit et al. (2004b) find that ZDI images of the very active primary star (G5 IV) in the HR 1099 system ($P_{\rm rot} = 2.84$ days) show that unlike HD 199178, the magnetic energy in the G5 IV star is mostly toroidal with changes seen in the smaller-scale structure on time scales of 4–6 weeks and has a much smaller differential rotation than the Sun. Since $\langle B_{\rm z} \rangle$ is only 40–120 Gauss, most of the photospheric energy is at smaller scales than ZDI can resolve. The rapid rotation and deep convective zones of these stars produce the strong dynamos that power the magnetic fields in these stars.

Single giants and supergiants show a diversity of magnetic properties. We list here five examples in order of increasing rotational period that exemplify this diversity as inferred from ZDI measurements. V390 Aur is a G5 III active star (strong Ca II and X-ray emission) with $P_{\rm rot} = 9.825$ days located at the base of the red giant branch (RGB). Konstantinova-Antova et al. (2012) find that this star has a moderately strong magnetic field $\langle B_{\rm z} \rangle$ that varies between $+2$ and -16 G with a strong toroidal component likely produced by an efficient $\alpha\Omega$ dynamo. β Cet is a somewhat more evolved K0 III star also located at the base of the RGB with $P_{\rm rot} = 215$ days. This star has an axisymmetric poloidal field dominated by a dipole. Tsvetkova et al. (2013) argue that this is a fossil field left over from when β Cet was an Ap star on the main sequence. Continuing to the more slowly rotating stars, we mention Pollux (β Gem), an inactive K0 III giant located in the RGB with $P_{\rm rot} \approx 590$ days. Aurière et al. (2009) find that this star has a weak, but measurable, $\langle B_{\rm z} \rangle = -0.46 \pm 0.04$ G that they suggest is produced by a weak $\alpha\Omega$ dynamo. EK Boo is an M5 III star with $P_{\rm rot} \approx 846$ days located at the tip of the RGB or on the asymptotic giant branch (AGB). Konstantinova-Antova et al. (2010) measure a variable $\langle B_{\rm z} \rangle$ between -0.1 and 8 G that could be produced by a weak $\alpha\Omega$ dynamo. Finally, Aurière et al. (2010) measured a magnetic field of about 1 G on the M2 Iab supergiant Betelgeuse (α Ori). With its very slow rotation period of about 17 years, this star's very weak field may be created by a local small-scale dynamo.

7 Conclusions

It is essential both to measure stellar magnetic fields and to understand what physical quantity is actually measured, because magnetic fields play many critical roles concerning the structure and energy balance in stellar atmospheres. These roles include creating the heat input in stellar chromospheres and coronae, controlling the mass and angular momentum loss from the star, facilitating chemical peculiarity, and energizing the emission of high-energy photons, which are critically important for the evolution of proto-planetary disks and the habitability of exoplanets. Since these effects are governed by the star's magnetic energy, which is proportional to the magnetic-field strength squared and its fractional surface coverage, it is essential to measure or credibly infer the true magnetic-field strength and filling factor across a stellar disk. Magnetic-field strengths and filling factors have been measured only for the Sun and then only with extreme care. We have indicated how and when it is feasible to estimate magnetic-field strengths for stars. There are now many examples for which the large-scale magnetic morphologies of stars have been inferred with ZDI techniques, but the small scale morphologies are matters of inference rather than measurement. The following points summarize our main conclusions:

Magnetic-Field Complexity and Cancellation Two critical questions that should be answered to understand any stellar magnetic-field measurement are (a) whether or not oppositely oriented magnetic fields cancel as detected by the observing instrument, and (b) whether or not the magnetic field has a complex structure across the surface of the star or in a spatial-resolution element for ZDI measurements. High-resolution spectra, especially in the infrared, but also in the optical for stars with very strong magnetic fields, measure the component of the magnetic field along the line of sight without cancellation from Zeeman broadening of absorption lines when the magnetic splitting is smaller than the intrinsic line width or Zeeman splitting when the field strength is large enough to separate the Zeeman pattern in wavelength compared to the intrinsic line width. On the other hand, all spectropolarimetric measurements include potential field cancellation. Except for the chemically peculiar A and B stars, most stars have complex magnetic-field structures that are unresolved by existing instruments. Therefore, most spectropolarimetric magnetic-field measurements will not measure true magnetic-field strengths. Field cancellation will be especially important for solar-like main sequence stars for which the Sun provides the test case of extreme complexity, but many other types of stars likely also have complex magnetic fields.

Magnetic Field Terminology We reserve the vector quantity "magnetic-field strength" for measurements in which the field is spatially resolved (or corrected for lack of resolution) without cancellation. We use the term "modulus" to refer to the peak magnetic-field strength. For spectral measurements with no cancellation, $B_{\rm MOD}$ refers to the "unsigned magnetic-field modulus", and for spectropolarimetric measurements in which there is field cancellation, $B_{\rm NET}$ refers to the "net magnetic-field modulus". When observing spectral lines that are Zeeman split, it is possible to separate out the corresponding "modulus" from the filling factor.

What Can Be Learned from the Sun? As the only star that can be spatially resolved, the Sun provides a unique test case for understanding the morphology and strength of a stellar magnetic field and how different observing techniques provide very different measurements of magnetic-field quantities. When observed as a star-like point source either in the light reflected by an asteroid or by co-adding all pixels in solar magnetograms, the net-longitudinal

magnetic-field strength $\langle B_z \rangle$ is at most ± 2 G at maximum activity and usually far less. By contract, high-spatial resolution spectropolarimetry of magnetically sensitive infrared lines with Zeeman splitting exceeding the line width reveals that the solar magnetic field is highly filamentary with magnetic-field modulus values in the range 1300–1600 G, in equipartition with the photospheric gas pressure, and very small filling factors of about 4.5 %. The magnetic energy of a 1600 G field covering 4.5 % of the solar surface is 1400 times larger than the energy content of a 2 Gauss field covering 100 % of the surface. Spatial averaging, even with subarcsecond-sized apertures, such as with the Solar Optical Telescope (SOT) instrument on the *HINODE* satellite, require correction for unresolved-magnetic structures to provide sensible estimates of the photospheric magnetic-field modulus and filling factor. Since stars with convective zones like the Sun, likely also have highly complex magnetic-field morphologies, one should expect that spectrophotometric observations will provide net magnetic-field strengths far smaller than the magnetic-field modulus because of cancellation in spatially unresolved observations. Only unpolarized spectra of magnetically split lines offer the possibility of measuring the stellar magnetic-field modulus and filling factor but without information on the magnetic-field morphology.

Pre-Main Sequence Stars Pre-main sequence stars have strong magnetic fields and small areas where accretion from the circumstellar disk along magnetic field lines impact their surface creating postshock hot gas observed as bright emission in the He I λ5876 and other lines. For most CTTSs, the accretion shock is co-spatial with strong radial magnetic fields at or near the magnetic poles and overlies dark starspots in the photosphere. The stellar magnetic field away from the accretion impact area can be approximated as a multipole with the octopole component often stronger than the dipole. For some CTTSs, the toroidal component of the field is comparable to, or even larger than, the poloidal component. As the higher mass CTTSs evolve toward the main sequence, they develop radiative cores and complex magnetic-field topologies leading to weaker magnetic dipoles and weaker interactions with their circumstellar disk. This evolution leads to a weakening of the star-disk deceleration torque and an increase in the stellar rotation rate as a result of the positive accretion torque and the decrease in stellar radius with age. Herbig Ae/Be stars are the higher mass analogs of the T Tauri stars with accretion from circumstellar disks and magnetic fields that are mostly dipolar and often inclined by large angles from the rotation axis. HD 101412 has the strongest net-longitudinal magnetic field ($\langle B_z \rangle = 3.5$ kG) yet measured for a Herbig Ae star.

Main-Sequence F–M Stars Main-sequence stars cooler than the Sun have complex magnetic fields with magnetic-field strengths and morphologies that depend systematically on spectral type and rotation period. Zeeman-broadening measurements show a pattern of increasing magnetic-field modulus, $B_{\rm MOD}$, with decreasing stellar mass, effective temperature, and rotation period. Magnetic-field modulus values correlate with commonly used indicators of magnetic heating and activity. For those stars in which Zeeman splitting is observed, the magnetic-field modulus and filling factor can be far larger than for the Sun. For example, the magnetic-field modulus and filling factor in the photosphere of the M3.5e star EV Lac were measured to be $B_{\rm MOD} = 3.8 \pm 0.5$ kG and $f = 0.50 \pm 0.13$. The corresponding magnetic energy per unit surface area is 50 times larger than for the Sun. Many M dwarf stars show similarly large $B_{\rm MOD}$ and f values. Most G–M dwarf stars have magnetic pressures close to equipartition with their nonmagnetic photospheric gas pressures and have filling factors that increase systematically with decreasing rotational period. ZDI provides information on the large-scale magnetic-field morphology, but ZDI images likely represent only a small fraction of the magnetic energy for these stars as a result of cancellation within each resolution

element. Unlike the Sun, cooler and more rapidly rotating dwarf stars have strong azimuthal fields that become stronger than poloidal fields for solar mass stars rotating faster than a 12-day period. Fully convective M dwarfs show a higher degree of magnetic field organization than higher mass stars as indicated by a lower degree of field cancellation. ZDI has provided evidence for changes in the large-scale magnetic morphology and even reversals in the poloidal magnetic field on yearly time scales. The very rapidly rotating K dwarf star AB Dor shows a magnetic field with a high percent of nonpotential magnetic energy in the photosphere and corona available for flaring.

Chemically Peculiar and Normal B-Type Stars Unlike cooler main sequence stars with convective zones, the chemically peculiar A- and B-type stars show magnetic-field structures that are organized on large scales–usually dipole or coaligned dipole, quadrupole, and octopole fields that are oriented at an angle with respect to the rotation axis. However, recent ZDI maps of the He-strong star HD 37776 show a magnetic topology that is too complex to be fit by a low-order multipole model. The three types of chemically peculiar stars, the magnetic Ap and Bp stars, metallic-line Am stars, and the HgMn stars, are often slow rotators compared to chemically normal stars with the same effective temperature. The CP stars are typically pre-main sequence stars or have just reached the main sequence with very strong magnetic fields that vary in rotational phase with the chemical peculiarities. The strongest magnetic-field modulus ever measured for a nondegenerate star is either for Babcock's star, $B_{\rm MOD} = 34$ kG, or for HD 37776, $B_{\rm MOD} = 43$–49 kG. Such strong magnetic fields control the winds and elemental abundance stratification of these stars. The magnetic fields of these stars are generally assumed to be primordial rather than dynamo generated and are strongest for the more massive and fastest rotating stars in this class. Unlike the chemically peculiar B-type stars, other B-type stars have either weak or undetected magnetic fields. Pulsating B stars of the β Cep and SPB classes have $\langle B_z \rangle \approx 400$ G or less. Be stars also have weak or undetected magnetic fields with $\langle B_z \rangle \approx 100$ G. The β Cephei star with the strongest longitudinal magnetic field (V1449 Aql) appears to have an oblique rotator magnetic structure.

O Stars The hottest main sequence stars, spectral types O and early-B, are not expected to have dynamo-generated magnetic fields because the stars do not have convective zones, but they could have "fossil" fields left over from the primordial nebulae out of which these stars recently formed or magnetic fields generated by strong tidal forces between binary stars. Spectrophotometric observations have detected magnetic fields for about two dozen O-type stars with net-longitudinal magnetic-field strengths generally less than 400 G. The O9.7 V star HD 54879 may be unusual with a dipole strength of 2 kG, and ζ Oph is a very rapidly rotating runaway star with a detected magnetic field. Some O-type stars show indirect evidence for magnetic fields including very high ionization states in X-ray spectra and very strong radio emission that can be explained by magnetic shocks in their massive winds.

Post-Main Sequence Stars As stars evolve off the main sequence, they expand, rotate more slowly, and, as a consequence, are expected to have weaker magnetic fields generated by their $\alpha\Omega$ dynamos. As stars progress up the red giant branch from subgiants to class-III red giants to M supergiants, their magnetic-flux measurements show a sequence of decreasing magnetic flux consistent with this picture. Their magnetic fields are assumed to be complex like their main-sequence predecessor stars, and poloidal or toroidal large-scale geometries have been detected in a few cases. Prominent exceptions to this decline in magnetic fields with evolution up the red giant branch are those close binaries whose rapid rotation

is enforced by tides leading to synchronized orbital and rotational periods. For the G or K-type subgiant or giant RS CVn systems and the FK Com stars, rapid rotation rejuvenates strong $\alpha\Omega$ dynamos leading to kG magnetic-field moduli detected by Zeeman-broadening techniques and toroidal magnetic-field morphologies detected by ZDI for the more rapidly rotating stars. In one case, HD 199178, ZDI measurements have detected remarkably rapid changes in the field morphology on a time scale of 4–6 weeks.

Acknowledgements We thank the referee for a careful reading of the manuscript and many useful suggestions. We thank the International Space Science Institute (ISSI) for their hospitality and the convenors of the ISSI workshop "The Strongest Magnetic Fields in the Universe" for organizing a stimulating workshop. JLL thanks the Space Telescope Science Institute for support of grants GO-12464 and GO-11616 to observe and analyze spectra of exoplanet host stars and premain sequence stars.

References

D.C. Abbott, J.H. Beiging, E. Churchwell, A.V. Torres, Radio emission from galactic Wolf–Rayet stars and the structure of Wolf–Rayet winds. Astrophys. J. **303**, 239–261 (1986). doi:10.1086/164070

F.C. Adams, S.G. Gregory, Magnetically controlled accretion flows onto young stellar objects. Astrophys. J. **744**, 55 (2012). doi:10.1088/0004-637X/744/1/55

E. Alecian, C. Catala, G.A. Wade, J.-F. Donati, P. Petit, J.D. Landstreet, T. Böhm, J.-C. Bouret, S. Bagnulo, C. Folsom, J. Grunhut, J. Silvester, Characterization of the magnetic field of the Herbig Be star HD200775. Mon. Not. R. Astron. Soc. **385**, 391–403 (2008). doi:10.1111/j.1365-2966.2008.12842.x

E. Alecian, G.A. Wade, C. Catala, S. Bagnulo, T. Böhm, J.-C. Bouret, J.-F. Donati, C.P. Folsom, J. Grunhut, J.D. Landstreet, Magnetism and binarity of the Herbig Ae star V380 Ori†. Mon. Not. R. Astron. Soc. **400**, 354–368 (2009). doi:10.1111/j.1365-2966.2009.15460.x

E. Alecian, C. Neiner, S. Mathis, C. Catala, O. Kochukhov, J. Landstreet, The dramatic change of the fossil magnetic field of HD 190073: evidence of the birth of the convective core in a Herbig star? Astron. Astrophys. **549**, 8 (2013). doi:10.1051/0004-6361/201220796

R.I. Anderson, A. Reiners, S.K. Solanki, On detectability of Zeeman broadening in optical spectra of F- and G-dwarfs. Astron. Astrophys. **522**, 81 (2010). doi:10.1051/0004-6361/201014769

M. Aurière, G.A. Wade, J. Silvester, F. Lignières, S. Bagnulo, K. Bale, B. Dintrans, J.-F. Donati, C.P. Folsom, M. Gruberbauer, A. Hui Bon Hoa, S. Jeffers, N. Johnson, J.D. Landstreet, A. Lèbre, T. Lueftinger, S. Marsden, D. Mouillet, S. Naseri, F. Paletou, P. Petit, J. Power, F. Rincon, S. Strasser, N. Toqué, Weak magnetic fields in Ap/Bp stars. Evidence for a dipole field lower limit and a tentative interpretation of the magnetic dichotomy. Astron. Astrophys. **475**, 1053–1065 (2007). doi:10.1051/0004-6361:20078189

M. Aurière, G.A. Wade, R. Konstantinova-Antova, C. Charbonnel, C. Catala, W.W. Weiss, T. Roudier, P. Petit, J.-F. Donati, E. Alecian, R. Cabanac, S. van Eck, C.P. Folsom, J. Power, Discovery of a weak magnetic field in the photosphere of the single giant Pollux. Astron. Astrophys. **504**, 231–237 (2009). doi:10.1051/0004-6361/200912050

M. Aurière, J.-F. Donati, R. Konstantinova-Antova, G. Perrin, P. Petit, T. Roudier, The magnetic field of Betelgeuse: a local dynamo from giant convection cells? Astron. Astrophys. **516**, 2 (2010). doi:10.1051/0004-6361/201014925

H.W. Babcock, Zeeman effect in stellar spectra. Astrophys. J. **105**, 105 (1947). doi:10.1086/144887

H.W. Babcock, The 34-KILOGAUSS magnetic field of HD 215441. Astrophys. J. **132**, 521 (1960). doi:10.1086/146960

S. Bagnulo, M. Landolfi, G. Mathys, M. Landi Degl'Innocenti, Modelling of magnetic fields of CP stars. III. The combined interpretation of five different magnetic observables: theory, and application to beta Coronae Borealis. Astron. Astrophys. **358**, 929–942 (2000)

S. Bagnulo, J.D. Landstreet, L. Fossati, O. Kochukhov, Magnetic field measurements and their uncertainties: the FORS1 legacy. Astron. Astrophys. **538**, 129–150 (2012). doi:10.1051/0004-6361/201118098

D. Baines, R.D. Oudmaijer, J.M. Porter, M. Pozzo, On the binarity of Herbig Ae/Be stars. Mon. Not. R. Astron. Soc. **367**, 737–753 (2006). doi:10.1111/j.1365-2966.2006.10006.x

P.K. Barker, J.M. Marlborough, J.D. Landstreet, I.B. Thompson, A search for magnetic fields in Be stars. Astrophys. J. **288**, 741–745 (1985). doi:10.1086/162841

J.H. Beiging, D.C. Abbott, E. Churchwell, A survey of radio emission from galactic OB stars. Astrophys. J. **340**, 518–536 (1989). doi:10.1086/167414

M. Benisty, K. Perraut, D. Mourard, P. Stee, G.H.R.A. Lima, J.B. Le Bouquin, M. Borges Fernandes, O. Chesneau, N. Nardetto, I. Tallon-Bosc, H. McAlister, T. Ten Brummelaar, S. Ridgway, J. Sturmann, L. Sturmann, N. Turner, C. Farrington, P.J. Goldfinger, Enhanced H activity at periastron in the young and massive spectroscopic binary HD 200775. Astron. Astrophys. **555**, 113 (2013). doi:10.1051/0004-6361/201219893

B.W. Bopp, S.H. Saar, C. Ambruster, P. Feldman, R. Dempsey, M. Allen, S.C. Barden, The active chromosphere binary HD 17433 (VY Arietis). Astrophys. J. **339**, 1059–1072 (1989). doi:10.1086/167360

J. Bouvier, S.H.P. Alencar, T.J. Harries, C.M. Johns-Krull, M.M. Romanova, Magnetospheric accretion in classical T Tauri stars, in *Protostars and Planets V*, ed. by B. Reipurth, D. Jewitt, K. Keil Protostars and Planets, vol. 5, 2007, pp. 479–494

M. Briquet, C. Neiner, B. Leroy, P.I. Pápics, Discovery of a magnetic field in the CoRoT hybrid B-type pulsator HD 43317. Astron. Astrophys. **557**, 16 (2013). doi:10.1051/0004-6361/201321779

C. Catala, E. Alecian, J.-F. Donati, G.A. Wade, J.D. Landstreet, T. Böhm, J.-C. Bouret, S. Bagnulo, C. Folsom, J. Silvester, The magnetic field of the pre-main sequence Herbig Ae star HD 190073. Astron. Astrophys. **462**, 293–301 (2007). doi:10.1051/0004-6361:20066264

W. Chen, C.M. Johns-Krull, Spectropolarimetry of the classical T Tauri star BP Tau. Astrophys. J. **776**, 113–132 (2013). doi:10.1088/0004-637X/776/2/113

C.R. Cowley, G.C.L. Aikman, Nuclear and nonnuclear abundance patterns in the manganese stars. Astrophys. J. **196**, 521–524 (1975). doi:10.1086/153432

C.R. Cowley, S. Hubrig, T.A. Ryabchikova, G. Mathys, N. Piskunov, P. Mittermayer, The core-wing anomaly of cool Ap stars. Abnormal Balmer profiles. Astron. Astrophys. **367**, 939–942 (2001). doi:10.1051/0004-6361:20000539

M. Cuntz, W. Rammacher, P. Ulmschneider, Z.E. Musielak, S.H. Saar, Two-component theoretical chromosphere models for K dwarfs of different magnetic activity: exploring the Ca II emission-stellar rotation relationship. Astrophys. J. **522**, 1053–1068 (1999). doi:10.1086/307689

A.G. Daou, C.M. Johns-Krull, J.A. Valenti, Spectropolarimetry of the classical T Tauri star T Tauri. Astron. J. **131**, 520–526 (2006). doi:10.1086/498306

J.-F. Donati, S.F. Brown, Zeeman–Doppler imaging of active stars. V. Sensitivity of maximum entropy magnetic maps to field orientation. Astron. Astrophys. **326**, 1135–1142 (1997)

J.-F. Donati, J.D. Landstreet, Magnetic fields of nondegenerate stars. Annu. Rev. Astron. Astrophys. **47**, 333–370 (2009). doi:10.1146/annurev-astro-082708-101833

J.-F. Donati, M. Semel, B.D. Carter, D.E. Rees, A. Collier Cameron, Spectropolarimetric observations of active stars. Mon. Not. R. Astron. Soc. **291**, 658 (1997)

J.-F. Donati, A. Collier Cameron, G.A.J. Hussain, M. Semel, Magnetic topology and prominence patterns on AB Doradus. Mon. Not. R. Astron. Soc. **302**, 437–456 (1999). doi:10.1046/j.1365-8711.1999.02095.x

J.-F. Donati, J. Babel, T.J. Harries, I.D. Howarth, P. Petit, M. Semel, The magnetic field and wind confinement of θ^1 Orionis C. Mon. Not. R. Astron. Soc. **333**, 55–70 (2002). doi:10.1046/j.1365-8711.2002.05379.x

J.-F. Donati, A. Collier Cameron, M. Semel, G.A.J. Hussain, P. Petit, B.D. Carter, S.C. Marsden, M. Mengel, A. López Ariste, S.V. Jeffers, D.E. Rees, Dynamo processes and activity cycles of the active stars AB Doradus, LQ Hydrae and HR 1099. Mon. Not. R. Astron. Soc. **345**, 1145–1186 (2003). doi:10.1046/j.1365-2966.2003.07031.x

J.-F. Donati, I.D. Howarth, J.-C. Bouret, P. Petit, C. Catala, J. Landstreet, Discovery of a strong magnetic field on the O star HD 191612: new clues to the future of θ^1 Orionis C*. Mon. Not. R. Astron. Soc. **365**, 6–10 (2006). doi:10.1111/j.1745-3933.2005.00115.x

J.-F. Donati, J. Morin, P. Petit, X. Delfosse, T. Forveille, M. Aurière, R. Cabanac, B. Dintrans, R. Fares, T. Gastine, M.M. Jardine, F. Lignières, F. Paletou, J.C. Ramirez Velez, S. Théado, Large-scale magnetic topologies of early M dwarfs. Mon. Not. R. Astron. Soc. **390**, 545–560 (2008a). doi:10.1111/j.1365-2966.2008.13799.x

J.-F. Donati, M.M. Jardine, S.G. Gregory, P. Petit, F. Paletou, J. Bouvier, C. Dougados, F. Ménard, A. Collier Cameron, T.J. Harries, G.A.J. Hussain, Y. Unruh, J. Morin, S.C. Marsden, N. Manset, M. Aurière, C. Catala, E. Alecian, Magnetospheric accretion on the T Tauri star BP Tauri. Mon. Not. R. Astron. Soc. **386**, 1234–1251 (2008b). doi:10.1111/j.1365-2966.2008.13111.x

J.-F. Donati, M.B. Skelly, J. Bouvier, M.M. Jardine, S.G. Gregory, J. Morin, G.A.J. Hussain, C. Dougados, F. Ménard, Y. Unruh, Complex magnetic topology and strong differential rotation on the low-mass T Tauri star V2247 Oph. Mon. Not. R. Astron. Soc. **402**, 1426–1436 (2010a). doi:10.1111/j.1365-2966.2009.15998.x

J.-F. Donati, M.B. Skelly, J. Bouvier, S.G. Gregory, K.N. Grankin, M.M. Jardine, G.A.J. Hussain, F. Ménard, C. Dougados, Y. Unruh, et al., Magnetospheric accretion and spin-down of the prototypical classical T Tauri star AA Tau. Mon. Not. R. Astron. Soc. **409**, 1347–1361 (2010b). doi:10.1111/j.1365-2966.2010.17409.x

J.-F. Donati, S.G. Gregory, S.H.P. Alencar, J. Bouvier, G.A.J. Hussain, M. Skelly, C. Dougados, M.M. Jardine, F. Ménard, C. Dougados, M.M. Romanova, et al., The large-scale magnetic field and poleward masss accretion of the classical T Tauri star TW Hya. Mon. Not. R. Astron. Soc. **417**, 472–487 (2011). doi:10.1111/j.1365-2966.2010.19288.x

J.-F. Donati, S.G. Gregory, S.H.P. Alencar, G.A.J. Hussain, J. Bouvier, M.M. Jardine, F. Ménard, C. Dougados, M.M. Romanova (the MaPP collaboration), Magnetospheric accretion on the fully convective classical T Tauri star DN Tau. Mon. Not. R. Astron. Soc. **436**, 881–897 (2013). doi:10.1093/mnras.436..881D

S. Edwards, W. Fischer, L. Hillenbrand, J. Kwan, Probing T Tauri accretion and outflow with 1 micron spectroscopy. Astrophys. J. **646**, 319–341 (2006). doi:10.1086/504832

V.G. Elkin, G. Mathys, D.W. Kurtz, S. Hubrig, L.M. Freyhammer, A rival for Babcock's star: 30-kG variable magnetic field in the Ap star HD 75049. Mon. Not. R. Astron. Soc. **402**, 1883–1891 (2010). doi:10.1111/j.1365-2966.2009.16015.x

E.D. Feigelson, T. Montmerle, High-energy processes in young stellar objects. Annu. Rev. Astron. Astrophys. **37**, 363–408 (1999). doi:10.1146/annurev.astro.37.1.363

L. Ferrario, A. Melatos, J. Zrake, Magnetic field generation in stars. Space Science Rev. (2015)

C.P. Folsom, G.A. Wade, O. Kochukhov, E. Alecian, C. Catala, S. Bagnulo, T. Böhm, J.-C. Bouret, J.-F. Donati, J. Grunhut, D.A. Hanes, J.D. Landstreet, Magnetic fields and chemical peculiarities of the very young intermediate-mass binary system HD 72106. Mon. Not. R. Astron. Soc. **391**, 901–914 (2008). doi:10.1111/j.1365-2966.2008.13946.x

L. Fossati, N. Castro, T. Morel, N. Langer, M. Briquet, T.A. Carroll, S. Hubrig, M.F. Nieva, L.M. Oskinova, N. Przybilla, F.R.N. Schneider, M. Schöller, S. Simón-Diaz, I. Ilyin, A. de Koter, A. Reisenegger, H. Sana (the BOB collaboration), B fields in OB stars (BOB): on the detection of weak magnetic fields in the two early B-type stars β CMa and ϵ CMa. Possible lack of a "magnetic desert" in massive stars. Astron. Astrophys. **574**, 20–34 (2015). doi:10.1051/0004-6361/201424986

C. Fourtune-Ravard, G.A. Wade, W.L.F. Marcolino, M. Shultz, J.H. Grunhut, H.F. Henrichs, (MiMeS Collaboration), The constant magnetic field of ξ^1 CMa: geometry or slow rotation? in *IAU Symposium*, ed. by C. Neiner, G. Wade, G. Meynet, G. Peters IAU Symposium, vol. 272, 2011, pp. 180–181. doi:10.1017/S1743921311010234

T. Gastine, J. Morin, L. Duarte, A. Reiners, U.R. Christensen, J. Wicht, What controls the magnetic geometry of M dwarfs? Astron. Astrophys. **549**, 5 (2013). doi:10.1051/0004-6361/201220317

T. Gatti, A. Natta, S. Randich, L. Testi, G. Sacco, Accretion properties of T Tauri stars in σ Orionis. Astron. Astrophys. **481**, 423–432 (2008). doi:10.1051/0004-6361:20078971

J.H. Grunhut, G.A. Wade, J.O. Sundqvist, A. ud-Doula, C. Neiner, R. Ignace, W.L.F. Marcolino, T. Rivinius, A. Fullerton, L. Kaper, B. Mauclaire, et al., Investigating the spectroscopic, magnetic and circumstellar variability of the O9 star HD 57682. Mon. Not. R. Astron. Soc. **426**, 2208–2227 (2012). doi:10.1111/j.1365-2966.2012.21799.x

F. Hamann, S.E. Persson, Emission-line studies of young stars. II. The Herbig Ae/Be stars. Astrophys. J. Suppl. Ser. **82**, 285 (1992). doi:10.1086/191716

S. Hubrig, N.V. Kharchenko, M. Schöller, The kinematic characteristics of magnetic O-type stars. Astron. Nachr. **332**, 65 (2011). doi:10.1002/asna.201011479

S. Hubrig, P. North, G. Mathys, Magnetic AP stars in the Hertzsprung–Russell diagram. Astrophys. J. **539**, 352–363 (2000). doi:10.1086/309189

S. Hubrig, L.M. Oskinova, M. Schöller, First detection of a magnetic field in the fast rotating runaway Oe star ζ Ophiuchi. Astron. Nachr. **332**, 147 (2011). doi:10.1002/asna.201111516

S. Hubrig, M. Schöller, R.V. Yudin, Magnetic fields in Herbig Ae stars. Astron. Astrophys. **428**, 1–4 (2004). doi:10.1051/0004-6361:200400091

S. Hubrig, N. Nesvacil, M. Schöller, P. North, G. Mathys, D.W. Kurtz, B. Wolff, T. Szeifert, M.S. Cunha, V.G. Elkin, Detection of an extraordinarily large magnetic field in the unique ultra-cool Ap star HD 154708. Astron. Astrophys. **440**, 37–40 (2005). doi:10.1051/0004-6361:200500164

S. Hubrig, R.V. Yudin, M. Schöller, M.A. Pogodin, Accurate magnetic field measurements of Vega-like stars and Herbig Ae/Be stars. Astron. Astrophys. **446**, 1089–1094 (2006a). doi:10.1051/0004-6361:20053794

S. Hubrig, M. Briquet, M. Schöller, P. De Cat, G. Mathys, C. Aerts, Discovery of magnetic fields in the βCephei star ξ^1 CMa and in several slowly pulsating B stars*. Mon. Not. R. Astron. Soc. **369**, 61–65 (2006b). doi:10.1111/j.1745-3933.2006.00175.x

S. Hubrig, M.A. Pogodin, R.V. Yudin, M. Schöller, R.S. Schnerr, The magnetic field in the photospheric and circumstellar components of Herbig Ae stars. Astron. Astrophys. **463**, 1039–1046 (2007). doi:10.1051/0004-6361:20066090

S. Hubrig, M. Schöller, R.S. Schnerr, J.F. González, R. Ignace, H.F. Henrichs, Magnetic field measurements of O stars with FORS 1 at the VLT. Astron. Astrophys. **490**, 793–800 (2008a). doi:10.1051/0004-6361:200810171

S. Hubrig, M. Briquet, T. Morel, M. Schöller, J.F. González, P. De Cat, New insights into the nature of the peculiar star θ Carinae. Astron. Astrophys. **488**, 287–296 (2008b). doi:10.1051/0004-6361:200809972

S. Hubrig, M. Schöller, I. Savanov, R.V. Yudin, M.A. Pogodin, S. Štefl, T. Rivinius, M. Curé, Magnetic survey of emission line B-type stars with FORS 1 at the VLT. Astron. Nachr. **330**, 708 (2009a). doi:10.1002/asna.200911236

S. Hubrig, M. Briquet, P. De Cat, M. Schöller, T. Morel, I. Ilyin, New magnetic field measurements of β Cephei stars and slowly pulsating B stars. Astron. Nachr. **330**, 317 (2009b). doi:10.1002/asna.200811187

S. Hubrig, B. Stelzer, M. Schöller, C. Grady, O. Schütz, M.A. Pogodin, M. Curé, K. Hamaguchi, R.V. Yudin, Searching for a link between the magnetic nature and other observed properties of Herbig Ae/Be stars and stars with debris disks. Astron. Astrophys. **502**, 283–301 (2009c). doi:10.1051/0004-6361/200811533

S. Hubrig, M. Schöller, I. Savanov, J.F. González, C.R. Cowley, O. Schütz, R. Arlt, G. Rüdiger, The exceptional Herbig Ae star HD 101412: the first detection of resolved magnetically split lines and the presence of chemical spots in a Herbig star. Astron. Nachr. **331**, 361 (2010). doi:10.1002/asna.201011346

S. Hubrig, M. Schöller, I. Ilyin, C.R. Cowley, Z. Mikulášek, B. Stelzer, M.A. Pogodin, R.V. Yudin, M. Curé, Characterising the magnetic fields of the Herbig Ae/Be stars HD 97048, HD 150193, HD 176386, and MWC 480. Astron. Astrophys. **536**, 45 (2011a). doi:10.1051/0004-6361/201117407

S. Hubrig, M. Schöller, N.V. Kharchenko, N. Langer, W.J. de Wit, I. Ilyin, A.F. Kholtygin, A.E. Piskunov, N. Przybilla (Magori Collaboration), Exploring the origin of magnetic fields in massive stars: a survey of O-type stars in clusters and in the field. Astron. Astrophys. **528**, 151 (2011b). doi:10.1051/0004-6361/201016345

S. Hubrig, I. Ilyin, M. Schöller, M. Briquet, T. Morel, P. De Cat, First magnetic field models for recently discovered magnetic β cephei and slowly pulsating B stars. Astrophys. J. Lett. **726**, 5 (2011c). doi:10.1088/2041-8205/726/1/L5

S. Hubrig, Z. Mikulášek, J.F. González, M. Schöller, I. Ilyin, M. Curé, M. Zejda, C.R. Cowley, V.G. Elkin, M.A. Pogodin, R.V. Yudin, Rotationally modulated variations and the mean longitudinal magnetic field of the Herbig Ae star HD 101412. Astron. Astrophys. **525**, 4 (2011d). doi:10.1051/0004-6361/201015806

S. Hubrig, I. Ilyin, M. Briquet, M. Schöller, J.F. González, N. Nuñez, P. De Cat, T. Morel, The strong magnetic field of the large-amplitude β Cephei pulsator V1449 Aquilae. Astron. Astrophys. **531**, 20 (2011e). doi:10.1051/0004-6361/201117261

S. Hubrig, F. Castelli, J.F. González, V.G. Elkin, G. Mathys, C.R. Cowley, B. Wolff, M. Schöller, Line identification in high-resolution, near-infrared CRIRES spectra of chemically peculiar and Herbig Ae stars. Astron. Astrophys. **542**, 31 (2012a). doi:10.1051/0004-6361/201218968

S. Hubrig, J.F. González, I. Ilyin, H. Korhonen, M. Schöller, I. Savanov, R. Arlt, F. Castelli, G. Lo Curto, M. Briquet, T.H. Dall, Magnetic fields of HgMn stars. Astron. Astrophys. **547**, 90 (2012b). doi:10.1051/0004-6361/201219778

S. Hubrig, M. Schöller, I. Ilyin, N.V. Kharchenko, L.M. Oskinova, N. Langer, J.F. González, A.F. Kholtygin, M. Briquet (Magori Collaboration), Exploring the origin of magnetic fields in massive stars. II. New magnetic field measurements in cluster and field stars. Astron. Astrophys. **551**, 33 (2013a). doi:10.1051/0004-6361/201220721

S. Hubrig, I. Ilyin, M. Schöller, G. Lo Curto, HARPS spectropolarimetry of Herbig Ae/Be stars. Astron. Nachr. **334**, 1093 (2013b). doi:10.1002/asna.201311948

S. Hubrig, L. Fossati, T.A. Carroll, N. Castro, J.F. González, I. Ilyin, N. Przybilla, M. Schöller, L.M. Oskinova, T. Morel, N. Langer, R.D. Scholz, N.V. Kharchenko, M.-F. Nieva, B fields in OB stars (BOB): the discovery of a magnetic field in a multiple system in the Trifid nebula, one of the youngest star forming regions. Astron. Astrophys. **564**, 10 (2014). doi:10.1051/0004-6361/201423490

G.A.J. Hussain, Stellar surface imaging: mapping brightness and magnetic fields. Astron. Nachr. **325**, 216–220 (2004). doi:10.1002/asna.200310219

G.A.J. Hussain, A.A. van Ballegooijen, M. Jardine, A. Collier Cameron, The coronal topology of the rapidly rotating K0 dwarf AB doradus. I. using surface magnetic field maps to model the structure of the stellar corona. Astrophys. J. **575**, 1078–1086 (2002). doi:10.1086/341429

G.A.J. Hussain, A. Collier Cameron, M.M. Jardine, N. Dunstone, J. Ramirez Velez, .C. Stempels, J.-F. Donati, M. Semel, G. Aulanier, T. Harries, et al., Surface magnetic fields on two accreting T Tauri stars: CV Cha and CR Cha. Mon. Not. R. Astron. Soc. **398**, 189–200 (2009). doi:10.1111/j.1365-2966.2009.14881.x

C.M. Johns-Krull, The magnetic fields of classical T Tauri stars. Astrophys. J. **664**, 975–985 (2007). doi:10.1086/519017

C.M. Johns-Krull, J.A. Valenti, Detection of strong magnetic fields on M Dwarfs. Astrophys. J. Lett. **459**, 95 (1996). doi:10.1086/309954

C.M. Johns-Krull, J.A. Valenti, A.P. Hatzes, A. Kanaan, Spectropolarimetry of magnetospheric accretion on the classical T Tauri star BP Tauri. Astrophys. J. **510**, 41–44 (1999). doi:10.1086/311802
C.M. Johns-Krull, T.P. Greene, G.W. Doppmann, K.R. Covey, First magnetic field detection on a class I Protostar. Astrophys. J. **700**, 1440–1448 (2009). doi:10.1088/0004-637X/700/2/1440
C.P. Johnstone, M. Jardine, S.G. Gregory, J.-F. Donati, G. Hussain, Classical T Tauri stars: magnetic fields, coronae and star-disk interactions. Mon. Not. R. Astron. Soc. **437**, 3202–3220 (2014). doi:10.1093/mnras/stt2107
E. Kambe, H. Ando, R. Hirata, Shortterm line-profile variations and episodic mass loss in the Be-Star Zeta-Ophiuchi. Astron. Astrophys. **273**, 435 (1993a)
E. Kambe, H. Ando, R. Hirata, G.A.H. Walker, E.J. Kennelly, J.M. Matthews, Line-profile variations of Lambda Eridani in emission and quiescence. Publ. Astron. Soc. Pac. **105**, 1222–1231 (1993b). doi:10.1086/133299
O. Kochukhov, G.A. Wade, Magnetic Doppler imaging of α^2 Canum Venaticorum in all four Stokes parameters: unveiling the hidden complexity of stellar magnetic fields. Astron. Astrophys. **513**, 13–25 (2010). doi:10.1051/0004-6361/2009113860
O. Kochukhov, S. Bagnulo, G.A. Wade, L. Sangalli, N. Piskunov, J.D. Landstreet, P. Petit, T.A.A. Sigut, Magnetic Doppler imaging of 53 Camelopardalis in all four Stokes parameters. Astron. Astrophys. **414**, 613–632 (2004). doi:10.1051/0004-6361:20031595
O. Kochukhov, A. Lundin, I. Romanyuk, D. Kudryavtsev, The extraordinary complex magnetic fields of the helium-strong star HD 37776. Astrophys. J. **726**, 24–31 (2011). doi:10.1088/0004-637X/726/1/24
O. Kochukhov, V. Makaganiuk, N. Piskunov, S.V. Jeffers, C.M. Johns-Krull, C.U. Keller, M. Rodenhuis, F. Snik, H.C. Stempels, J.A. Valenti, Are there tangled magnetic fields on HgMn stars? Astron. Astrophys. **554**, 61 (2013). doi:10.1051/0004-6361/201321467
L. Kohoutek, P. Mayer, R. Lorenz, Photometry and spectroscopy of the central star of the Trifid nebula. Astron. Astrophys. Suppl. Ser. **134**, 129–133 (1999). doi:10.1051/aas:1999128
R. Konstantinova-Antova, M. Aurière, C. Charbonnel, N.A. Drake, K.-P. Schröder, I. Stateva, E. Alecian, P. Petit, R. Cabanac, Direct detection of a magnetic field in the photosphere of the single M giant EK Bootis. How common is magnetic activity among M giants? Astron. Astrophys. **524**, 57 (2010). doi:10.1051/0004-6361/201014503
R. Konstantinova-Antova, M. Aurière, P. Petit, C. Charbonnel, S. Tsvetkova, A. Lèbre, R. Bogdanovski, Magnetic field structure in single late-type giants: the effectively single giant V390 Aurigae. Astron. Astrophys. **541**, 44 (2012). doi:10.1051/0004-6361/201116690
M. Landolfi, S. Bagnulo, M. Landi Degl'Innocenti, Modelling of magnetic fields of CP stars I. A diagnostic method for dipole and quadrupole fields from Stokes I and V observations. Astron. Astrophys. **338**, 111–121 (1998)
J.D. Landstreet, G. Mathys, Magnetic models of slowly rotating magnetic Ap stars: aligned magnetic and rotation axes. Astron. Astrophys. **359**, 213–226 (2000)
J.D. Landstreet, S. Bagnulo, L. Fossati, On the consistency of magnetic field measurements of Ap stars: lessons learned from the FORS1 archive. Astron. Astrophys. **572**, 113–125 (2014). doi:10.1051/0004-6361/201424749
J.D. Landstreet, S. Bagnulo, V. Andretta, L. Fossati, E. Mason, J. Silaj, G.A. Wade, Searching for links between magnetic fields and stellar evolution II. The evolution of magnetic fields as revealed by observations of Ap stars in open clusters and associations. Astron. Astrophys. **470**, 685–698 (2007). doi:10.1051/0004-6361:20077343
P. Lang, M. Jardine, J. Morin, J.-F. Donati, S. Jeffers, A.A. Vidotto, R. Fares, Modelling the hidden magnetic field of low-mass stars. Mon. Not. R. Astron. Soc. **439**, 2122–2131 (2014). doi:10.1093/mnras/stu091
C. Leinert, A. Richichi, M. Haas, Binaries among Herbig Ae/Be stars. Astron. Astrophys. **318**, 472–484 (1997)
J.L. Leroy, Linear polarimetry of AP stars. V. A general catalogue of measurements. Astron. Astrophys. Suppl. Ser. **114**, 79 (1995)
J.L. Leroy, S. Bagnulo, M. Landolfi, E. Landi Degl'Innocenti, A long period model for the magnetic star gamma Equulei. Astron. Astrophys. **284**, 174–178 (1994)
J.L. Linsky, S.A. Drake, T.S. Bastian, Radio emission from chemically peculiar stars. Astrophys. J. **393**, 341–356 (1992). doi:10.1086/171509
T. Lüftinger, O. Kochukhov, T. Ryabchikova, N. Piskunov, W.W. Weiss, I. Ilyin, Magnetic Doppler imaging of the roAp star HD 24712. Astron. Astrophys. **509**, 71 (2010). doi:10.1051/0004-6361/200811545
G.W. Marcy, G. Basri, Physical realism in the analysis of stellar magnetic fields. II—K dwarfs. Astrophys. J. **345**, 480–488 (1989). doi:10.1086/167921
F. Martins, J.-F. Donati, W.L.F. Marcolino, J.-C. Bouret, G.A. Wade, C. Escolano, I.D. Howarth (Mimes Collaboration), Detection of a magnetic field on HD108: clues to extreme magnetic braking and the Of?p phenomenon. Mon. Not. R. Astron. Soc. **407**, 1423–1432 (2010). doi:10.1111/j.1365-2966.2010.17005.x

G. Mathys, Spectropolarimetry of magnetic stars. II—The mean longitudinal magnetic field. Astron. Astrophys. Suppl. Ser. **89**, 121–157 (1991)
G. Mathys, Magnetic field diagnosis through spectropolarimetry, in *IAU Colloq. 138: Peculiar Versus Normal Phenomena in A-Type and Related Stars*, ed. by M.M. Dworetsky, F. Castelli, R. Faraggiana Astronomical Society of the Pacific Conference Series, vol. 44, 1993, p. 232
G. Mathys, Spectropolarimetry of magnetic stars. IV. The crossover effect. Astron. Astrophys. **293**, 733–745 (1995a)
G. Mathys, Spectropolarimetry of magnetic stars. V. The mean quadratic magnetic field. Astron. Astrophys. **293**, 746–763 (1995b)
G. Mathys, S. Hubrig, J.D. Landstreet, T. Lanz, J. Manfroid, The mean magnetic field modulus of AP stars. Astron. Astrophys. Suppl. Ser. **123**, 353–402 (1997). doi:10.1051/aas:1997103
C.F. McKee, E.C. Ostriker, Theory of star formation. Annu. Rev. Astron. Astrophys. **45**, 565–687 (2007). doi:10.1146/annurev.astro.45.051806.110602
Y.-J. Moon, Y.-H. Kim, Y.-D. Park, K. Ichimoto, T. Sakurai, J. Chae, K.S. Cho, S. Bong, Y. Suematsu, S. Tsuneta, Y. Katsukawa, M. Shimojo, T. Shimizu, R.A. Shine, T.D. Tarbell, A.M. Title, B. Lites, M. Kubo, S. Nagata, T. Yokoyama, Hinode SP vector magnetogram of AR10930 and its cross-comparison with MDI. Publ. Astron. Soc. Jpn. **59**, 625 (2007). doi:10.1093/pasj/59.sp3.S625
T. Morel, N. Castro, L. Fossati, S. Hubrig, N. Langer, N. Przybilla, M. Schöller, T. Carroll, I. Ilyin, A. Irrgang, L. Oskinova, F. Schneider, S. Simon Díaz, M. Briquet, J.-F. González, N. Kharchenko, M.-F. Nieva, R.-D. Scholz, A. de Koter, W.-R. Hamann, A. Herrero, J. Maíz Apellániz, H. Sana, R. Arlt, R. Barbá, P. Dufton, A. Kholtygin, G. Mathys, A. Piskunov, A. Reisenegger, H. Spruit, S.-C. Yoon, The B Fields in OB Stars (BOB) Survey (2014)
A. Morgenthaler, P. Petit, S. Saar, S.K. Solanki, J. Morin, S.C. Marsden, M. Aurière, B. Dintrans, R. Fares, T. Gastine, J. Lanoux, F. Lignières, F. Paletou, J.C. Ramírez Vélez, S. Théado, V. Van Grootel, Long-term magnetic field monitoring of the Sun-like star ξ Bootis A. Astron. Astrophys. **540**, 138 (2012). doi:10.1051/0004-6361/201118139
J. Morin, J.-F. Donati, P. Petit, X. Delfosse, T. Forveille, L. Albert, M. Aurière, R. Cabanac, B. Dintrans, R. Fares, T. Gastine, M.M. Jardine, F. Lignières, F. Paletou, J.C. Ramirez Velez, S. Théado, Large-scale magnetic topologies of mid M dwarfs. Mon. Not. R. Astron. Soc. **390**, 567–581 (2008). doi:10.1111/j.1365-2966.2008.13809.x
J. Morin, J.-F. Donati, P. Petit, X. Delfosse, T. Forveille, M.M. Jardine, Large-scale magnetic topologies of late M dwarfs. Mon. Not. R. Astron. Soc. **407**, 2269–2286 (2010). doi:10.1111/j.1365-2966.2010.17101.x
Y. Nazé, A. Ud-Doula, M. Spano, G. Rauw, M. De Becker, N.R. Walborn, New findings on the prototypical Of?p stars. Astron. Astrophys. **520**, 59 (2010). doi:10.1051/0004-6361/201014333
C. Neiner, A.-M. Hubert, Y. Frémat, M. Floquet, S. Jankov, O. Preuss, H.F. Henrichs, J. Zorec, Rotation and magnetic field in the Be star omega Orionis. Astron. Astrophys. **409**, 275–286 (2003). doi:10.1051/0004-6361:20031086
N.J. Nelson, B.P. Brown, A.S. Brun, M.S. Miesch, J. Toomre, Magnetic wreaths and cycles in convective dynamos. Astrophys. J. **762**, 73–92 (2013). doi:10.1088/0004-637X/762/73
N.J. Nelson, B.P. Brown, A.S. Brun, M.S. Miesch, J. Toomre, Buoyant magnetic loops generated by global convective action. Sol. Phys. **289**, 441–458 (2014). doi:10.1007/s11207-012-0221-4
B. Nordstrom, K.T. Johansen, Radii and masses for young star AR Aurigae. Astron. Astrophys. **282**, 787–800 (1994)
M.E. Oksala, G.A. Wade, R.H.D. Townsend, S.P. Owocki, O. Kochukhov, C. Neiner, E. Alecian, J. Grunhut (the MiMeS Collaboration), Revisiting the rigidly rotating magnetosphere model for σ Ori E—I. Observations and data analysis. Mon. Not. R. Astron. Soc. **419**, 959–970 (2012). doi:10.1111/j.1365-2966.2011.19753.x
P. Petit, J.-F. Donati, G.A. Wade, J.D. Landstreet, S. Bagnulo, T. Lüftinger, T.A.A. Sigut, S.L.S. Shorlin, S. Strasser, M. Aurière, J.M. Oliveira, Magnetic topology and surface differential rotation on the K1 subgiant of the RS CVn system HR 1099. Mon. Not. R. Astron. Soc. **348**, 1175–1190 (2004a). doi:10.1111/j.1365-2966.2004.07420.x
P. Petit, J.-F. Donati, J.M. Oliveira, M. Aurière, S. Bagnulo, J.D. Landstreet, F. Lignières, T. Lüftinger, S. Marsden, D. Mouillet, F. Paletou, S. Strasser, N. Toqué, G.A. Wade, Photospheric magnetic field and surface differential rotation of the FK Com star HD 199178. Mon. Not. R. Astron. Soc. **351**, 826–844 (2004b). doi:10.1111/j.1365-2966.2004.07827.x
P. Petit, B. Dintrans, S.K. Solanki, J.-F. Donati, M. Aurière, F. Lignières, J. Morin, F. Paletou, J. Ramirez Velez, C. Catala, R. Fares, Toroidal versus poloidal magnetic fields in Sun-like stars: a rotation threshold. Mon. Not. R. Astron. Soc. **388**, 80–88 (2008). doi:10.1111/j.1365-2966.2008.13411.x
P. Petit, B. Dintrans, A. Morgenthaler, V. Van Grootel, J. Morin, J. Lanoux, M. Aurière, R. Konstantinova-Antova, A polarity reversal in the large-scale magnetic field of the rapidly rotating sun HD 190771. Astron. Astrophys. **508**, 9–12 (2009). doi:10.1051/0004-6361/200913285

V. Petit, S.P. Owocki, G.A. Wade, D.H. Cohen, J.O. Sundqvist, M. Gagné, J. Maíz Apellániz, M.E. Oksala, D.E. Bohlender, T. Rivinius, H.F. Henrichs, E. Alecian, R.H.D. Townsend, A. ud-Doula (MiMeS Collaboration), A magnetic confinement versus rotation classification of massive-star magnetospheres. Mon. Not. R. Astron. Soc. **429**, 398–422 (2013). doi:10.1093/mnras/sts344

A.A. Pevtsov, L. Bertello, A.G. Tlatov, A. Kilcik, Y.A. Nagovitsyn, E.W. Cliver, Cyclic and long-term variation of sunspot magnetic fields. Sol. Phys. **289**, 593–602 (2014). doi:10.1007/s11207-012-0220-5

N. Piskunov, O. Kochukhov, Doppler imaging of stellar magnetic fields. I. Techniques. Astron. Astrophys. **381**, 736–756 (2002). doi:10.1051/0004-6361:20011517

S. Plachinda, N. Pankov, D. Baklanova, General magnetic field of the Sun as a star (GMF): variability of the frequency spectrum from cycle to cycle. Astron. Nachr. **332**, 918 (2011). doi:10.1002/asna.201111591

S.I. Plachinda, T.N. Tarasova, Magnetic field variations with a rotational period on solar-like star ξ Bootis A. Astrophys. J. **533**, 1016–1022 (2000). doi:10.1086/308694

S.I. Plachinda, C.M. Johns-Krull, T.N. Tarasova, Direct measurements of the general magnetic field on the solar-like stars, in *Odessa Astronomical Publications* vol. 14 (2001), p. 219

D. Rabin, A true-field magnetogram in a solar plage region. Astrophys. J. Lett. **390**, 103–106 (1992). doi:10.1086/186382

A. Reiners, Observations of cool-star magnetic fields. Living Rev. Sol. Phys. **9**, 1 (2012). doi:10.12942/lrsp-2012-1

A. Reiners, G. Basri, The first direct measurements of surface magnetic fields on very low mass stars. Astrophys. J. **656**, 1121–1135 (2007). doi:10.1086/510304

A. Reiners, G. Basri, A volume-limited sample of 63 M7-M9.5 dwarfs. II. Activity, magnetism, and the fade of the rotation-dominated dynamo. Astrophys. J. **710**, 924–935 (2010). doi:10.1088/0004-637X/710/2/924

B. Reipurth, J. Bally, C. Aspin, M.S. Connelley, T.R. Geballe, S. Kraus, I. Appenzeller, A. Burgasser, HH 222: a giant herbig-haro flow from the quadruple system V380 Ori. Astron. J. **146**, 118 (2013). doi:10.1088/0004-6256/146/5/118

T. Rivinius, R.H.D. Townsend, O. Kochukhov, S. Stefl, D. Baade, L. Barrera, T. Szeifert, Basic parameters and properties of the rapidly rotating magnetic helium-strong B star HR 7355. Mon. Not. R. Astron. Soc. **429**, 177–188 (2013). doi:10.1093/mnras/sts323

R.D. Robinson, S.P. Worden, J.W. Harvey, Observations of magnetic fields on two late-type dwarf stars. Astrophys. J. Lett. **236**, 155–158 (1980). doi:10.1086/183217

J. Robrade, J.H.M.M. Schmitt, Altair—the "hottest" magnetically active star in X-rays. Astron. Astrophys. **497**, 511–520 (2009). doi:10.1051/0004-6361/200811348

J. Robrade, J.H.M.M. Schmitt, New X-ray observations of IQ Aurigae and α^2 Canum Venaticorum. Probing the magnetically channeled wind shock model in A0p stars. Astron. Astrophys. **531**, 58–68 (2011). doi:10.1051/0004-6361/201116843

M.M. Romanova, G.V. Ustyugova, A.V. Koldoba, J.V. Wick, R.V.E. Lovelace, Three-dimensional simulations of disk accretion to an inclined dipole. I. Magnetospheric flows at different Θ. Astrophys. J. **595**, 1009–1031 (2003). doi:10.1086/377514

C. Rossi, L. Errico, M. Friedjung, F. Giovannelli, G. Muratorio, R. Viotti, A. Vittone, On the nature of the Herbig Be star V 380 Orionis. Astron. Astrophys. Suppl. Ser. **136**, 95–105 (1999). doi:10.1051/aas:1999200

N. Rusomarov, O. Kochukhov, N. Piskunov, S.V. Jeffers, C.M. Johns-Krull, C.U. Keller, V. Makaganiuk, M. Rodenhuis, F. Snik, H.C. Stempels, J.A. Valenti, Three-dimensional magnetic and abundance mapping of the cool Ap star HD 24712 I. Spectropolarimetric observations in all four Stokes parameters. Astron. Astrophys. **558**, 8–23 (2013). doi:10.1051/0004-6361/201220950

S.H. Saar, Improved methods for the measurement and analysis of stellar magnetic fields. Astrophys. J. **324**, 441–465 (1988). doi:10.1086/165907

S.H. Saar, Recent magnetic fields measurements of stellar, in *Stellar Surface Structure*, ed. by K.G. Strassmeier, J.L. Linsky IAU Symposium, vol. 176, 1996, p. 237

S.H. Saar, J.L. Linsky, The photospheric magnetic field of the dM3.5e flare star AD Leonis. Astrophys. J. Lett. **299**, 47–50 (1985). doi:10.1086/184578

R.S. Schneer, H.F. Henrichs, R.D. Oudmaijer, J.H. Telting, On the Halpha emission from the beta Cephei system. Astron. Astrophys. **459**, 21–24 (2006). doi:10.1051/0004-6361:20066392

C.J. Schrijver, Y. Liu, The global solar magnetic field through a full sunspot cycle: observations and model results. Sol. Phys. **252**, 19–31 (2008). doi:10.1007/s11207-008-9240-6

C.J. Schrijver, C. Zwaan, *Solar and Stellar Magnetic Activity* (Cambridge University Press, Cambridge, 2000)

N.S. Schulz, C.R. Canizares, D. Huenemoerder, J.C. Lee, X-ray line emission from the hot stellar wind of θ^1 Ori C. Astrophys. J. **545**, 135–139 (2000). doi:10.1086/317891

M. Semel, Zeeman–Doppler imaging of active stars. I—Basic principles. Astron. Astrophys. **225**, 456–466 (1989)

D. Shulyak, A. Seifahrt, A. Reiners, O. Kochukhov, N. Piskunov, Rotation, magnetism and metallicity of M dwarf systems. Mon. Not. R. Astron. Soc. **418**, 2548–2557 (2011). doi:10.1111/j.1365-2966.2011.19644.x

J. Silvester, O. Kochukhov, G.A. Wade, Stokes IQUV magnetic Doppler imaging of Ap stars—III. Next generation chemical abundance mapping of α^2 CVn. Mon. Not. R. Astron. Soc. **444**, 1442–1452 (2014a). doi:10.1093/mnras/stu1531

J. Silvester, O. Kochukhov, G.A. Wade, Stokes IQUV magnetic Doppler imaging of Ap stars—II. Next generation magnetic Doppler imaging of α^2 CVn. Mon. Not. R. Astron. Soc. **440**, 182–192 (2014b). doi:10.1093/mnras/stu306

J. Silvester, C. Neiner, H.F. Henrichs, G.A. Wade, V. Petit, E. Alecian, A.-L. Huat, C. Martayan, J. Power, O. Thizy, On the incidence of magnetic fields in slowly pulsating B, Beta Cehpei and B-type emission line stars. Mon. Not. R. Astron. Soc. **398**, 1505–1511 (2009). doi:10.1111/j.1365-2966.2009.15208.x

J. Silvester, G.A. Wade, O. Kochukov, S. Bagnulo, C.P. Folsom, D. Hanes, Stokes IQUV magnetic Doppler imaging of Ap stars—I. ESPaDOnS and NARVAL observations. Mon. Not. R. Astron. Soc. **426**, 1003–1030 (2012). doi:10.1111/j.1365-2966.2012.21587.x

M.A. Smith, Photospheric activity in selected Be stars: lambda ERI and gamma CAS, in *Pulsation; Rotation; and Mass Loss in Early-Type Stars*, ed. by L.A. Balona, H.F. Henrichs, J.M. Le Contel IAU Symposium, vol. 162, 1994, p. 241

B. Stelzer, G. Micela, K. Hamaguchi, J.H.M.M. Schmitt, On the origin of the X-ray emission from Herbig Ae/Be stars. Astron. Astrophys. **457**, 223–235 (2006). doi:10.1051/0004-6361:20065006

T. Szeifert, S. Hubrig, M. Schöller, O. Schütz, B. Stelzer, Z. Mikulášek, The nature of the recent extreme outburst of the Herbig Be/FU Orionis binary Z Canis Majoris. Astron. Astrophys. **509**, 7 (2010). doi:10.1051/0004-6361/200913704

N. Tetzlaff, R. Neuhäuser, M.M. Hohle, G. Maciejewski, Identifying birth places of young isolated neutron stars. Mon. Not. R. Astron. Soc. **402**, 2369–2387 (2010). doi:10.1111/j.1365-2966.2009.16093.x

S. Tsvetkova, P. Petit, M. Aurière, R. Konstantinova-Antova, G.A. Wade, C. Charbonnel, T. Decressin, R. Bogdanovski, Magnetic field structure in single late-type giants: β Ceti in 2010–2012. Astron. Astrophys. **556**, 43 (2013). doi:10.1051/0004-6361/201321051

J.A. Valenti, C. Johns-Krull, Magnetic field measurements for cool stars, in *Magnetic Fields Across the Hertzsprung–Russell Diagram*, ed. by G. Mathys, S.K. Solanki, D.T. Wickramasinghe The Astronomical Society of the Pacific Conference Series, vol. 248, 2001, p. 179

J.A. Valenti, G.W. Marcy, G. Basri, Infrared Zeeman analysis of epsilon Eridani. Astrophys. J. **439**, 939–956 (1995). doi:10.1086/175231

A.A. Vidotto, S.G. Gregory, M. Jardine, J.-F. Donati, P. Petit, J. Morin, C.P. Folsom, J. Bouvier, A.C. Cameron, G. Hussain, S. Marsden, I.A. Waite, R. Fares, S. Jeffers, J.D. do Nascimento Jr, Stellar magnetism: empirical trends with age and rotation. Mon. Not. R. Astron. Soc. **441**, 2361–2374 (2014). doi:10.1093/mnras/stu728

B. Viticchié, J. Sánchez Almeida, D. Del Moro, F. Berrilli, Interpretation of HINODE SOT/SP asymmetric Stokes profiles observed in the quiet Sun network and internetwork. Astron. Astrophys. **526**, 60 (2011). doi:10.1051/0004-6361/201015391

S.S. Vogt, G.D. Penrod, Doppler imaging of spotted stars—application to the RS Canum venaticorum star HR 1099. Publ. Astron. Soc. Pac. **95**, 565–576 (1983). doi:10.1086/131208

G.A. Wade, the MiMeS Collaboration, Review: Magnetic fields of O-type stars (2014). arXiv:1411.3604

G.A. Wade, J.H. Grunhut (MiMeS Collaboration), The MiMeS survey of magnetism in massive stars, in *Circumstellar Dynamics at High Resolution*, ed. by A.C. Carciofi, T. Rivinius Astronomical Society of the Pacific Conference Series, vol. 464, 2012, p. 405

G.A. Wade, D. Drouin, S. Bagnulo, J.D. Landstreet, E. Mason, J. Silvester, E. Alecian, T. Böhm, J.-C. Bouret, C. Catala, J.-F. Donati, Discovery of the pre-main sequence progenitors of the magnetic Ap/Bp stars? Astron. Astrophys. **442**, 31–34 (2005). doi:10.1051/0004-6361:200500184

G.A. Wade, S. Bagnulo, D. Drouin, J.D. Landstreet, D. Monin, A search for strong, ordered magnetic fields in Herbig Ae/Be stars. Mon. Not. R. Astron. Soc. **376**, 1145–1161 (2007). doi:10.1111/j.1365-2966.2007.11495.x

G.A. Wade, J. Maíz Apellániz, F. Martins, V. Petit, J. Grunhut, N.R. Walborn, R.H. Barbá, M. Gagné, E. García-Melendo, J. Jose, A.F.J. Moffat, Y. Nazé, C. Neiner, A. Pellerin, M. Penadés Ordaz, M. Shultz, S. Simón-Díaz, A. Sota, NGC 1624-2: a slowly rotating, X-ray luminous Of?cp star with an extraordinarily strong magnetic field. Mon. Not. R. Astron. Soc. **425**, 1278–1293 (2012a). doi:10.1111/j.1365-2966.2012.21523.x

G.A. Wade, J. Grunhut, G. Gräfener, I.D. Howarth, F. Martins, V. Petit, J.S. Vink, S. Bagnulo, C.P. Folsom, Y. Nazé, N.R. Walborn, R.H.D. Townsend, C.J. Evans, The spectral variability and magnetic field characteristics of the Of?p star HD 148937. Mon. Not. R. Astron. Soc. **419**, 2459–2471 (2012b). doi:10.1111/j.1365-2966.2011.19897.x

N.R. Walborn, The space distribution of the O stars in the solar neighborhood. Astron. J. **78**, 1067–1073 (1973). doi:10.1086/111509

G.A.H. Walker, R. Kuschnig, J.M. Matthews, P. Reegen, T. Kallinger, E. Kambe, H. Saio, P. Harmanec, D.B. Guenther, A.F.J. Moffat, S.M. Rucinski, D. Sasselov, W.W. Weiss, D.A. Bohlender, H. Božić, O. Hashimoto, P. Koubský, R. Mann, D. Ruždjak, P. Škoda, M. Šlechta, D. Sudar, M. Wolf, S. Yang, Pulsations of the Oe star ζ ophiuchi from MOST satellite photometry and ground-based spectroscopy. Astrophys. J. Lett. **623**, 145–148 (2005). doi:10.1086/430254

H. Yang, C.M. Johns-Krull, Magnetic field measurements of T Tauri stars in the Orion Nebula Cluster. Astrophys. J. **729**, 83–90 (2011). doi:10.1088/004-637X/729/2/83

H. Yang, C.M. Johns-Krull, J.A. Valenti, Magnetic properties of young stars in the TW Hydrae Association. Astron. J. **136**, 2286–2294 (2008). doi:10.1088/0004-6256/136/6/2286